

Chapter 19

Endocrine and neuroendocrine tumors

19.1 Papillary carcinoma, gross features.



© El Bolkainy et al, Pathology of Cancer 2013

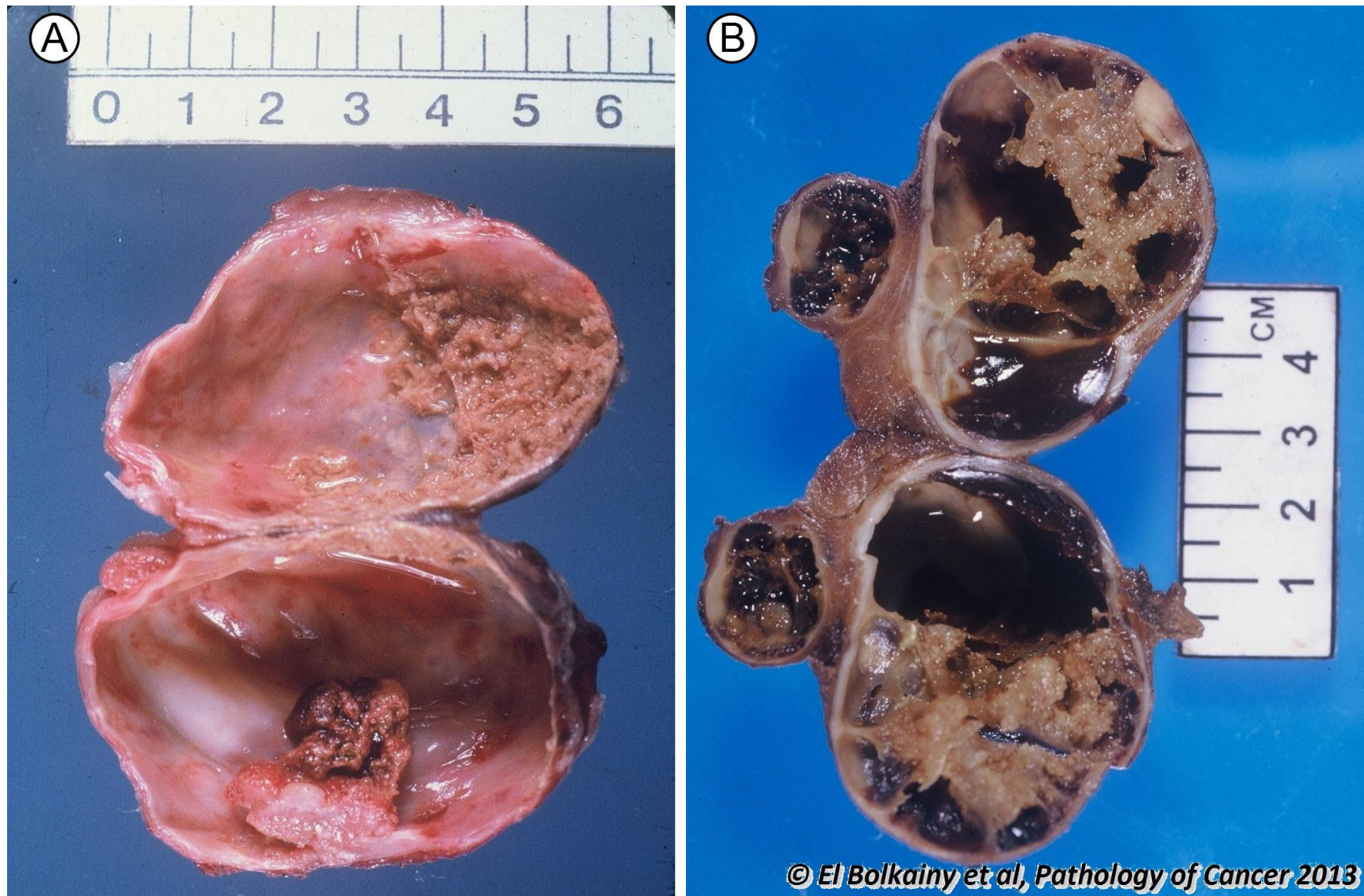
Picture 19-1 Papillary carcinoma, gross features. A unifocal encapsulated type. Note the circumscribed appearance with gray-white, granular non-shining cut surface. Thyroid capsule is intact.

19.2 Papillary carcinoma of thyroid, gross features.



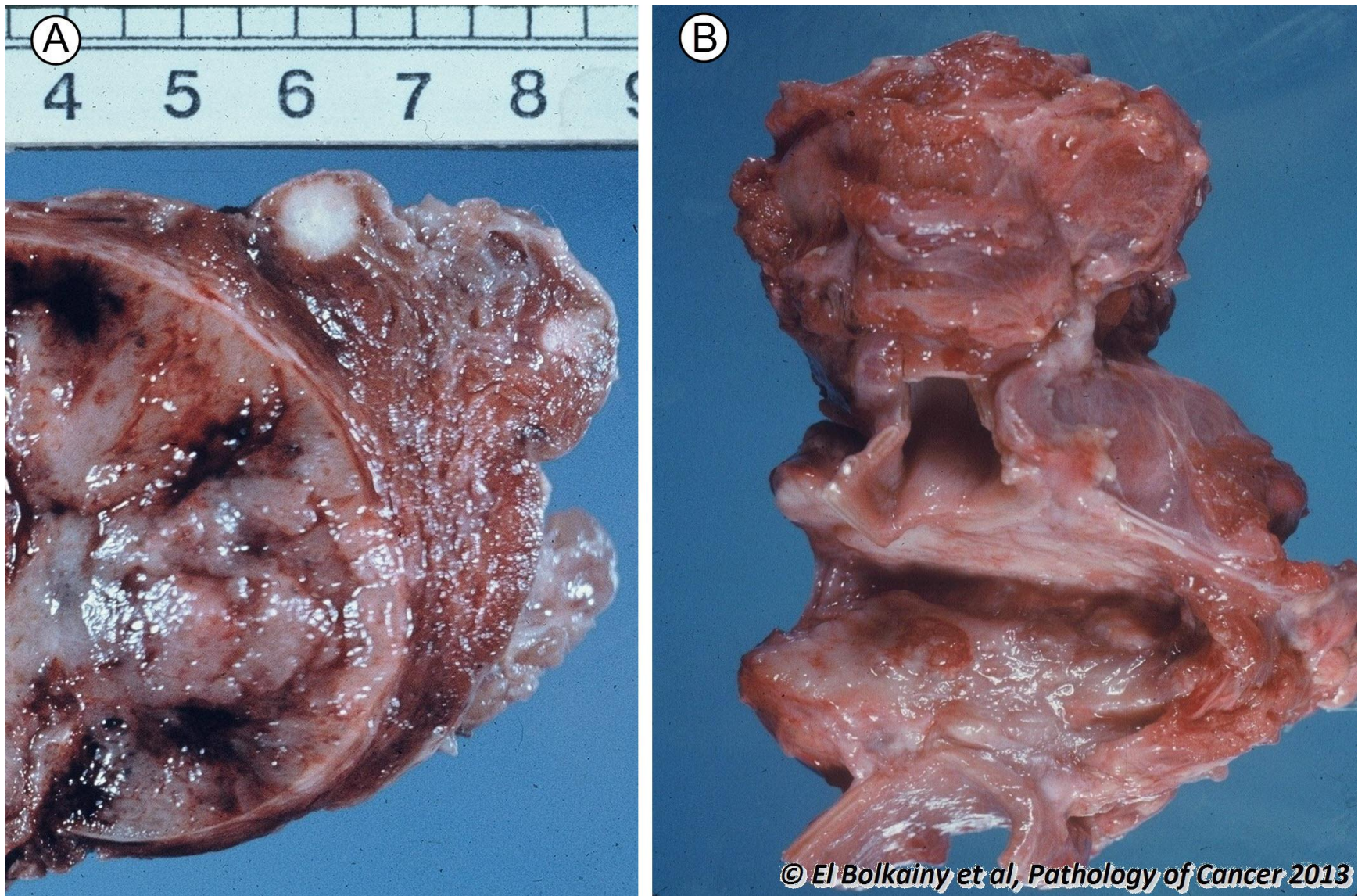
Picture 19-2 Papillary carcinoma of thyroid, gross features. A whitish fibrotic tumor with ill-defined infiltrative margins . There is associated lymph node metastases.

19.3 Papillary carcinoma, gross features.



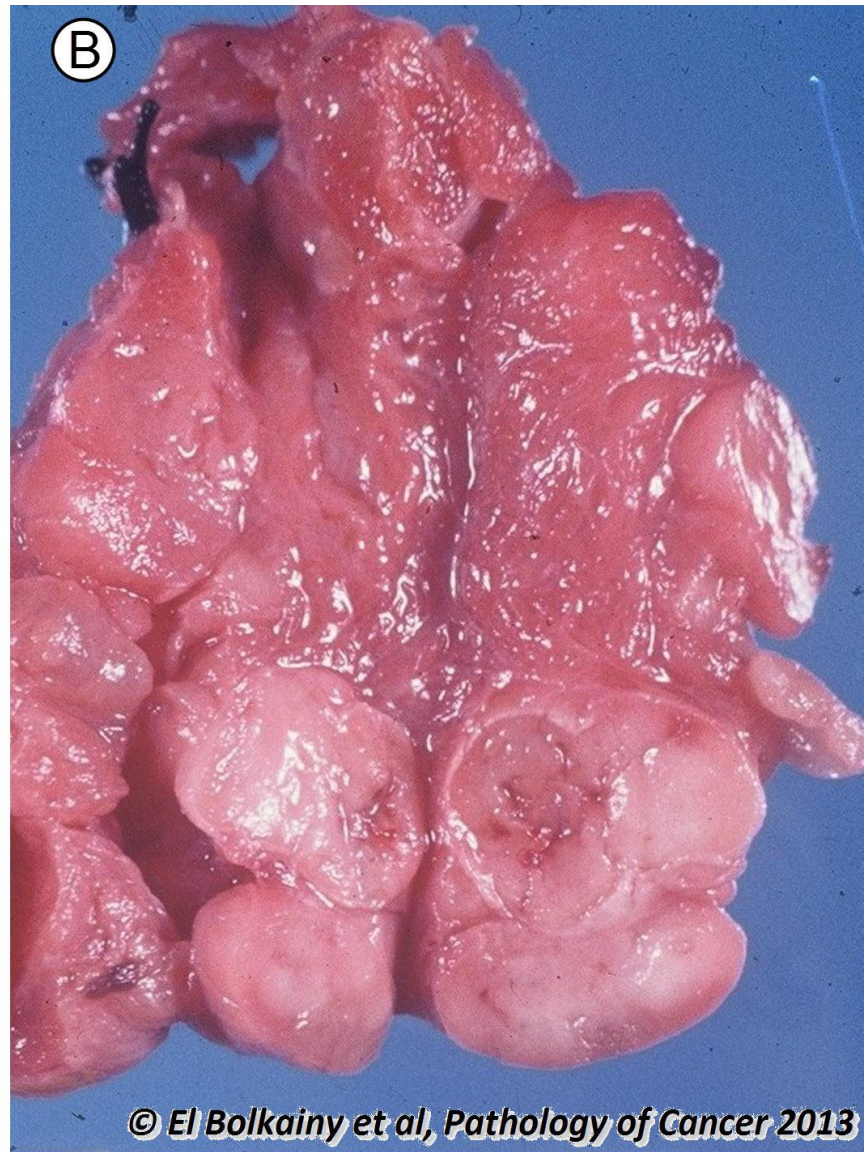
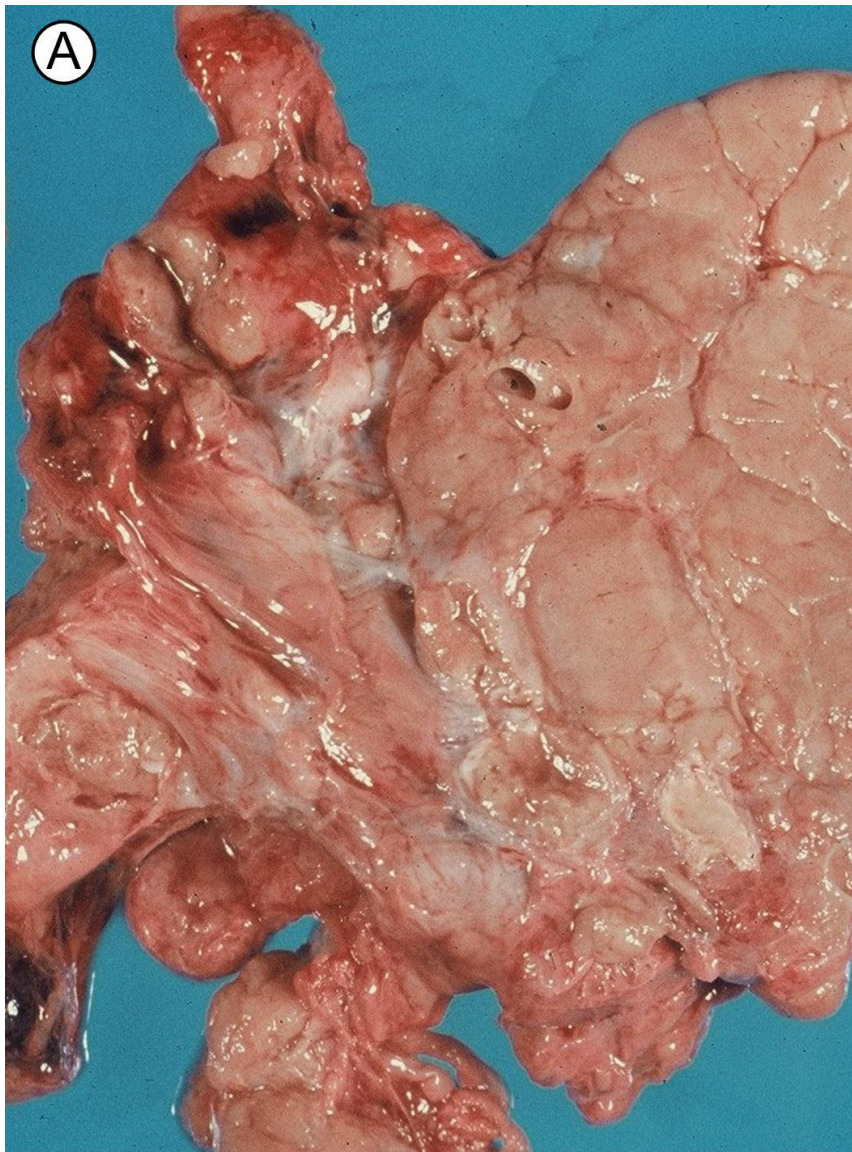
Picture 19-3 Papillary carcinoma, gross features. **A** Cystic carcinoma with mural papillary tumor attached to the cyst wall. **B** Lymph node metastases with marked cystic change, may be misdiagnosed as simple cysts.

19.4 Papillary carcinoma, gross features.



Picture 19-4 Papillary carcinoma, gross features. **A** A micro-carcinoma (5mm) associated with a benign adenoma with hemorrhage and cystic change. **B** Advanced thyroid carcinoma with extrathyroid spread and invasion of trachea (T4A).

19.5 Follicular carcinoma of thyroid, gross features.

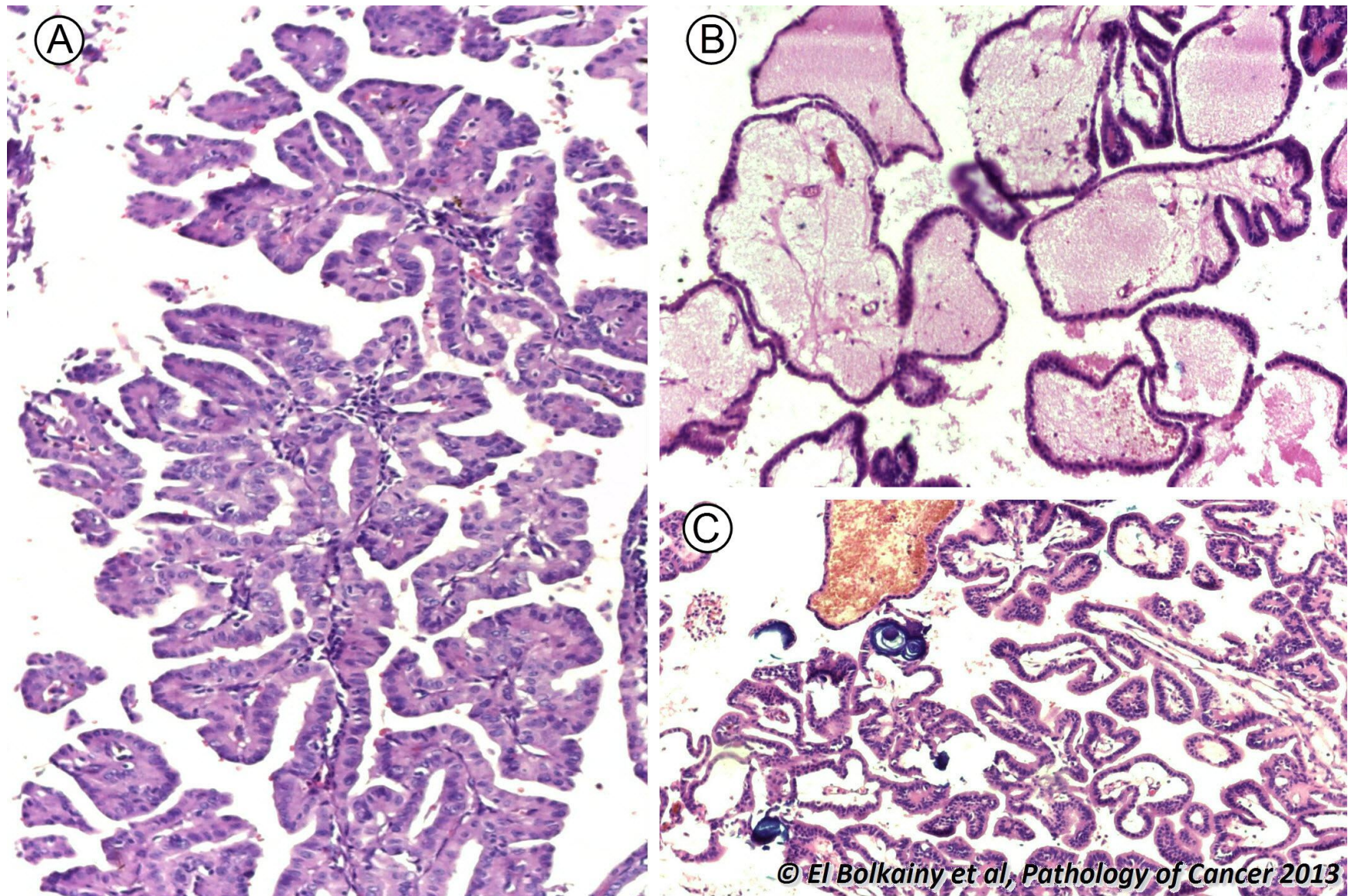


© El Bolkainy et al, Pathology of Cancer 2013

Picture Follicular carcinoma of thyroid, gross features. **A** Widely invasive type affecting most of thyroid lobe.

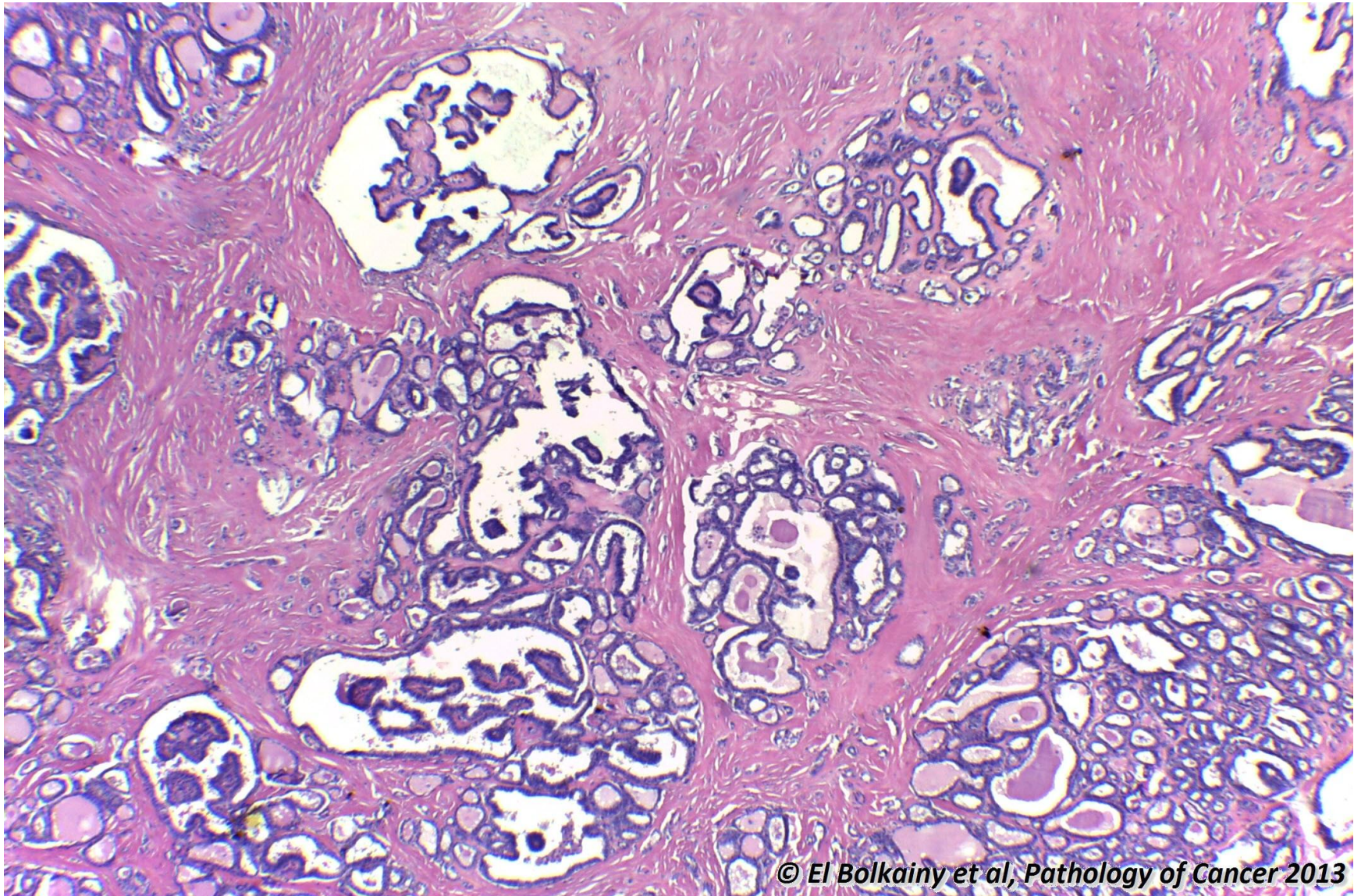
19-5 **B** Associated regional lymph node metastases.

19.6 Papillary carcinoma, histology.



Picture 19-6 Papillary carcinoma, histology. **A** Classic papillary pattern. **B** Large edematous papillae with fibrotic stroma. **C** Associated psammoma bodies (concentric microcalcification) are characteristic of this tumor.

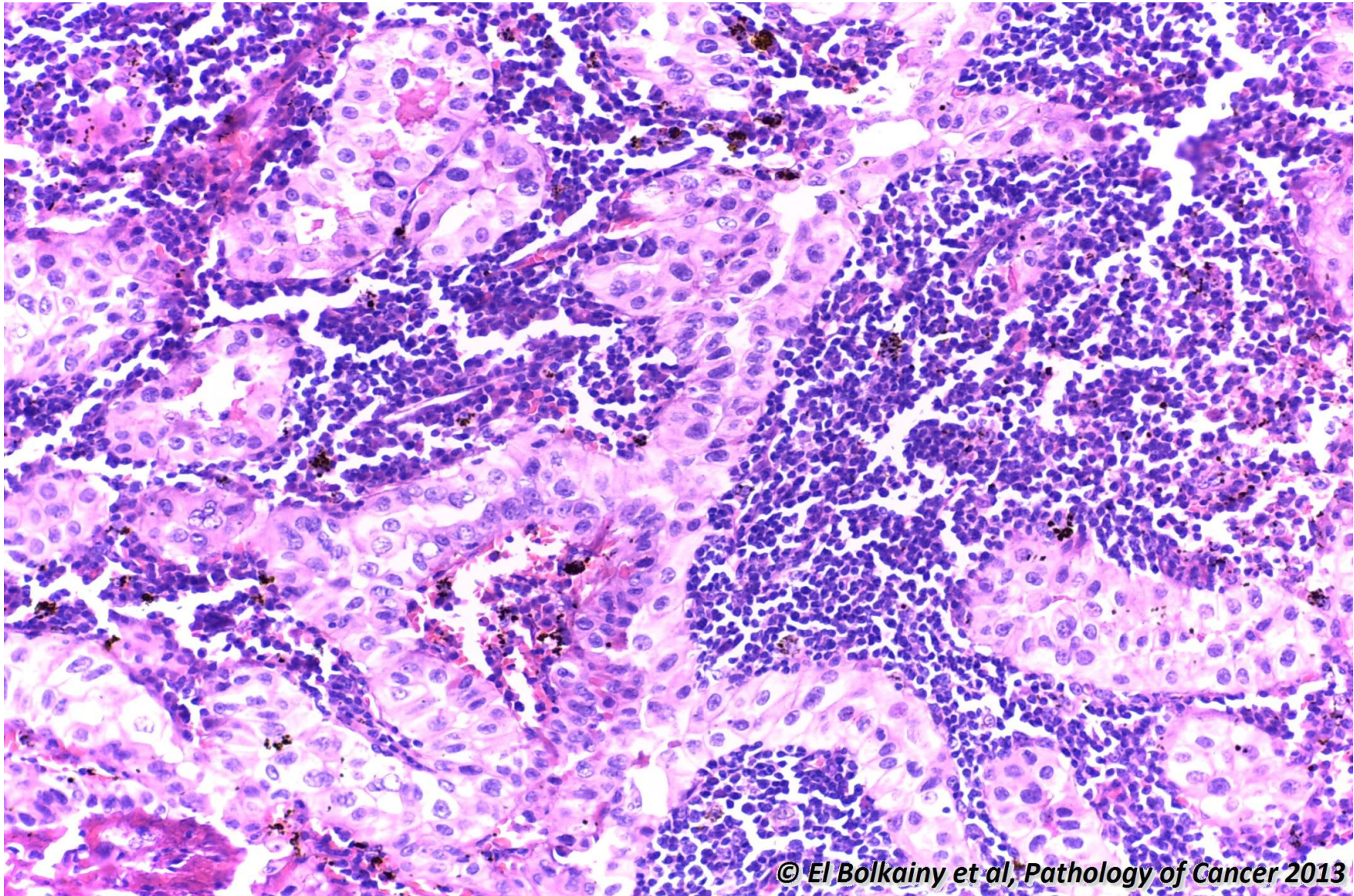
19.7 Papillary carcinoma, histology of sclerosing variant.



© El Bolkainy et al, Pathology of Cancer 2013

Picture 19-7 Papillary carcinoma, histology of sclerosing variant. Nests of carcinoma cells separated by dense fibrotic stroma (desmoplasia). This variant is usually of small size (5-10mm).

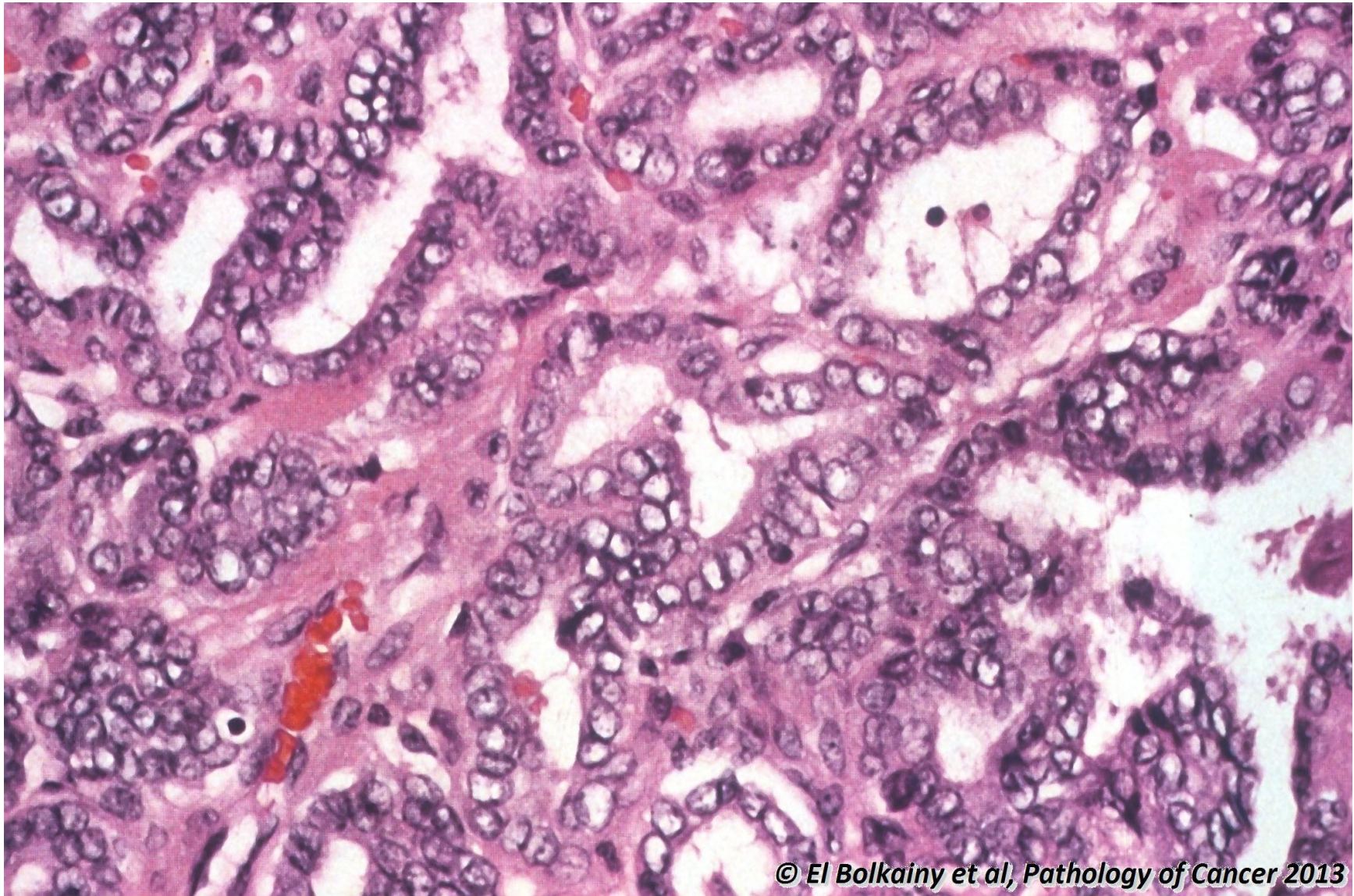
19.8 Papillary carcinoma, histology of oncocytic trabecular variant.



© El Bolkainy et al, Pathology of Cancer 2013

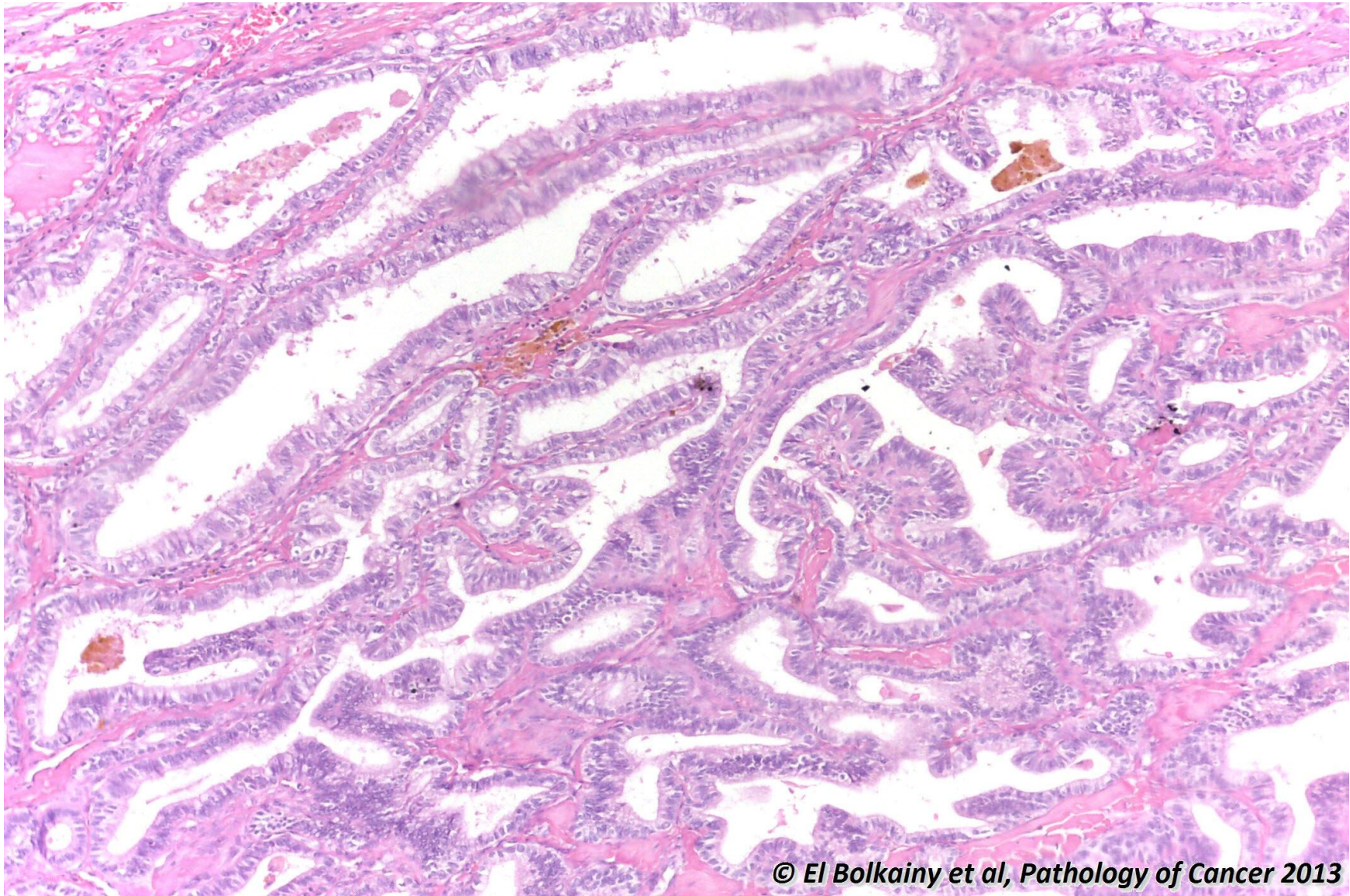
Picture 19-8 Papillary carcinoma, histology of oncocytic trabecular variant. The carcinoma cells have a pale eosinophilic cytoplasm, arranged in a trabecular pattern infiltrating thyroid, simulating metastases. Lymphocytes are common in the stroma.

19.9 Papillary carcinoma, histology of the follicular variant.



Picture 19-9 Papillary carcinoma, histology of the follicular variant. It is distinguished from a true follicular carcinoma by its clear nuclei (due to cytoplasmic inclusions) with grooves.

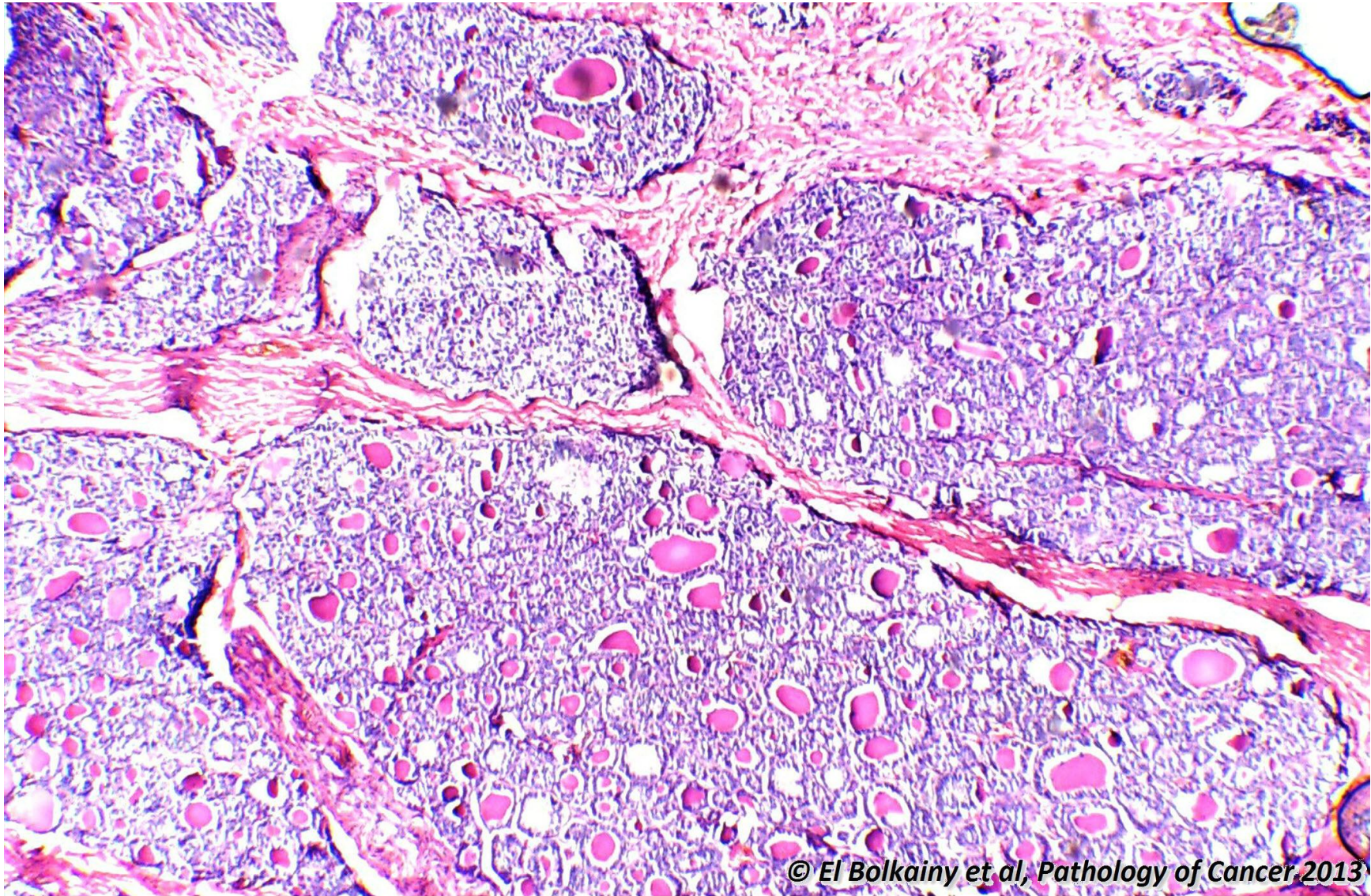
19.10 Papillary carcinoma, histology of the tall cell variant.



© El Bolkainy et al, Pathology of Cancer 2013

Picture 19-10 Papillary carcinoma, histology of the tall cell variant. Follicles and papillae are covered by very tall columnar cells (cell height 3 times its width). Its prognosis is less favorable than the classic papillary type, due to high tendency to disseminate. Fibrosis in stroma and squamous metaplasia may be observed.

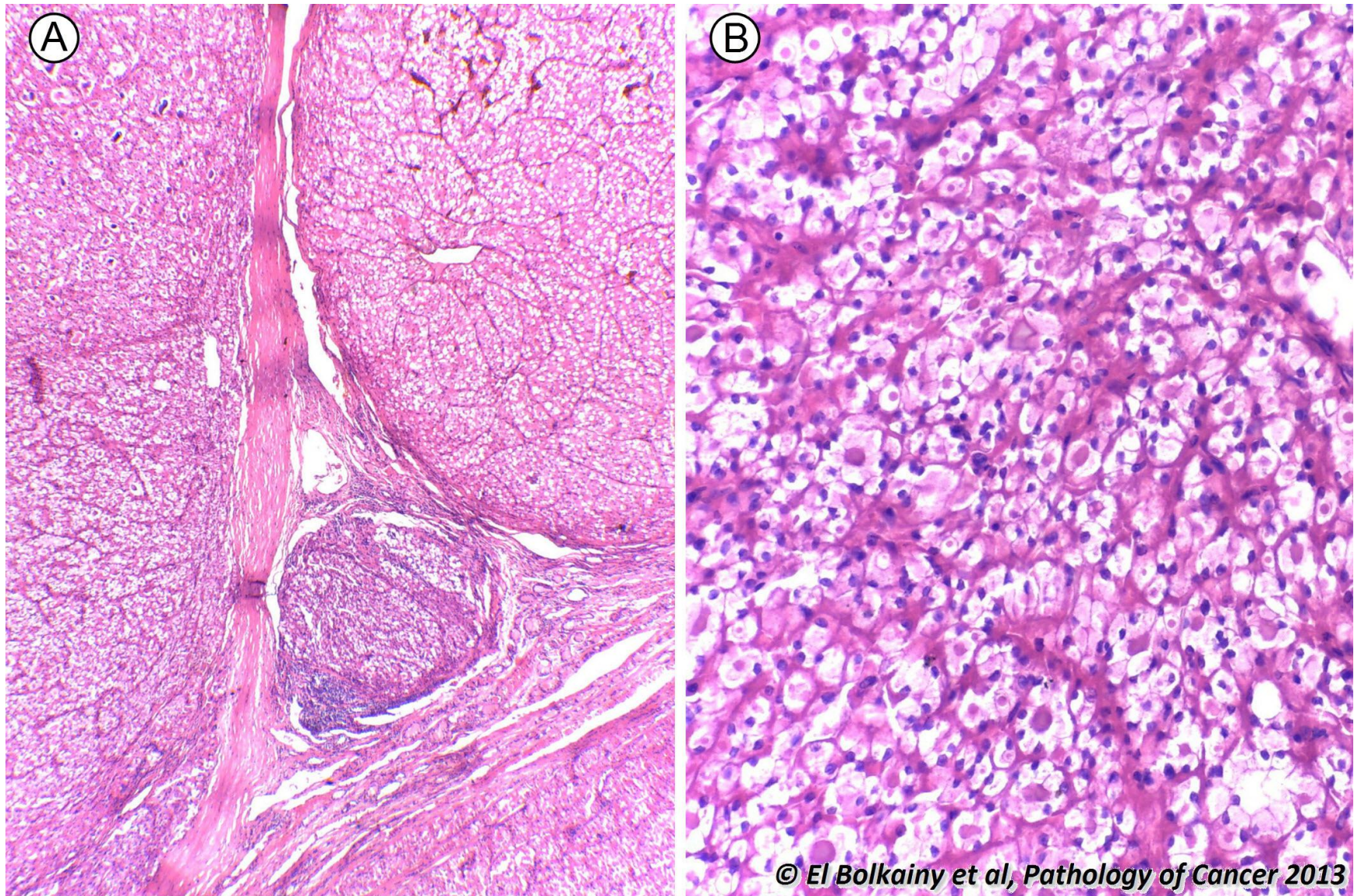
19.11 Follicular carcinoma, histology of widely invasive subtype.



© El Bolkainy et al, Pathology of Cancer, 2013

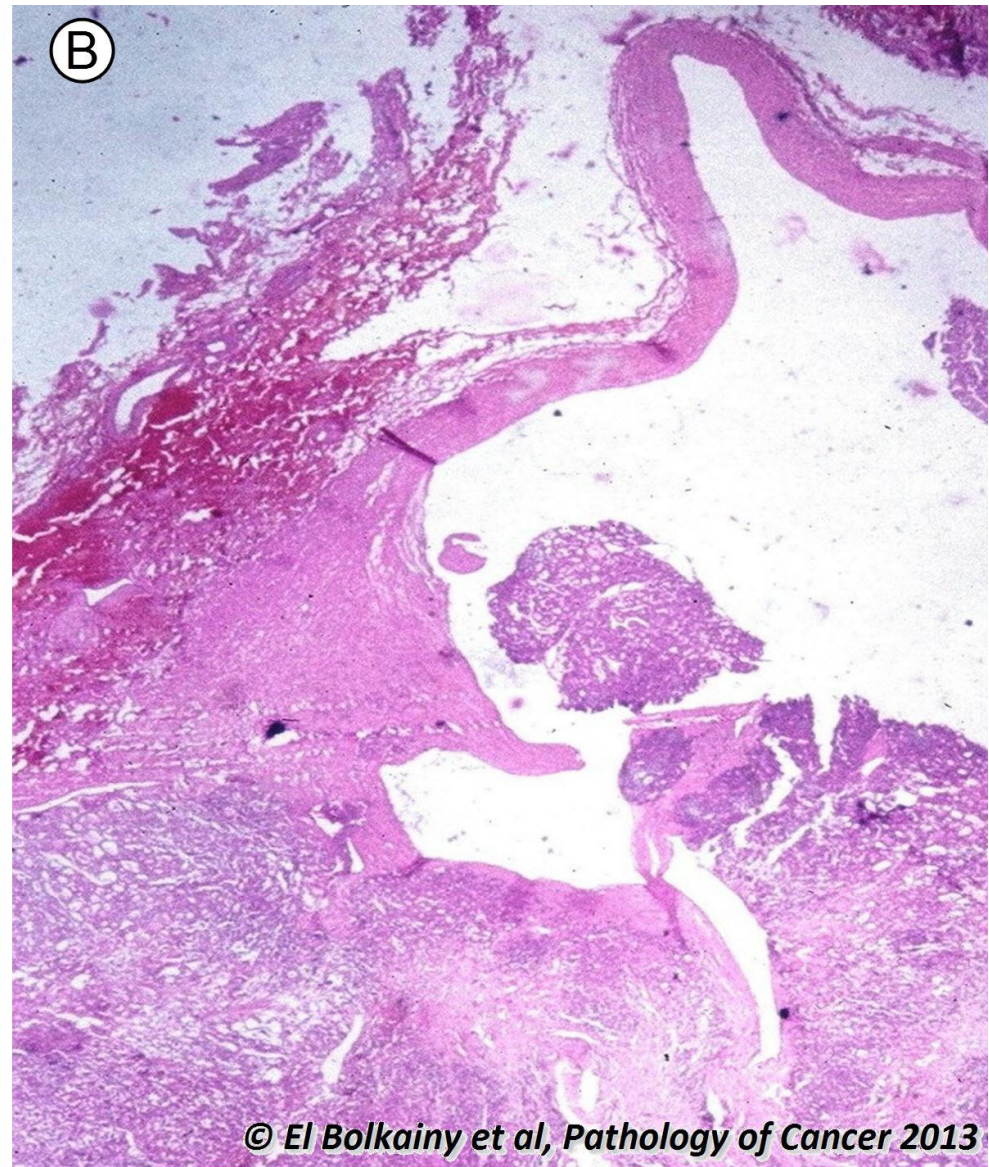
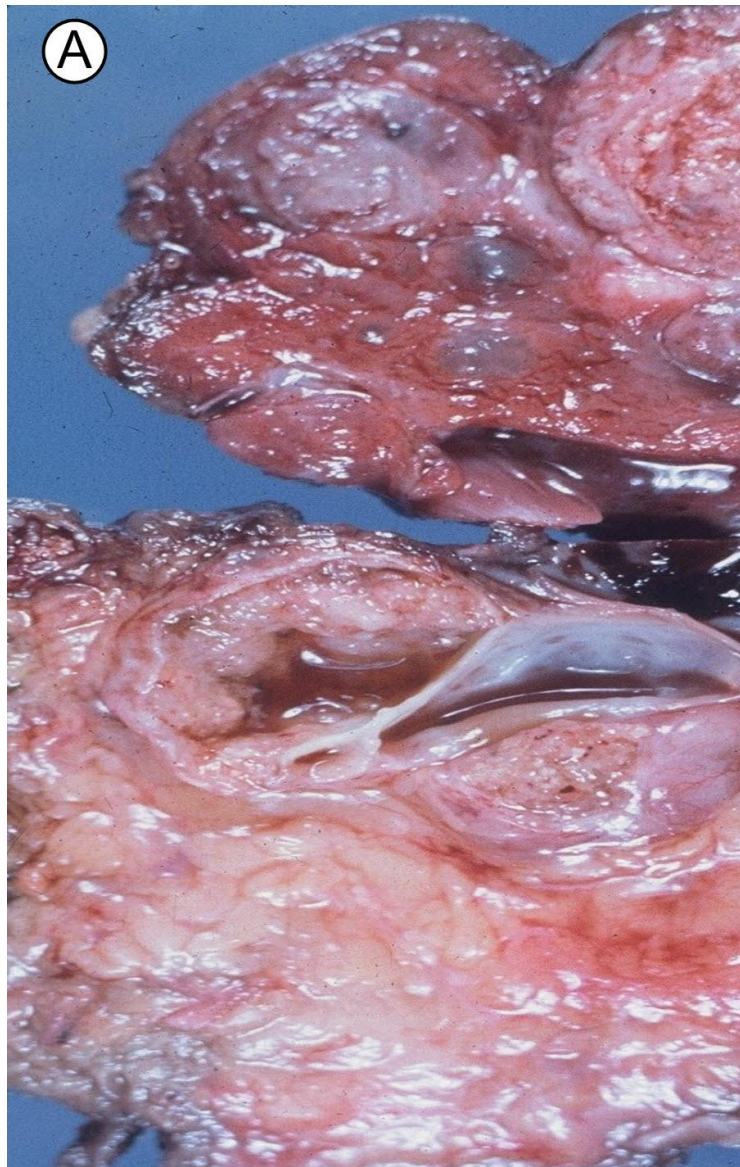
Picture 19-11 Follicular carcinoma, histology of widely invasive subtype. The carcinoma invades the capsule, as well as, thyroid tissue. Malignant follicles appear elongated rather than rounded, lined by crowded overlapping cells of variable size.

19.12 Follicular carcinoma, histology of clear cell variant.



Picture 19-12 Follicular carcinoma, histology of clear cell variant. The cytoplasm of tumor cells is clear. This must not be misdiagnosed as clear cell metastases in thyroid. **A** Low power. **B** High power.

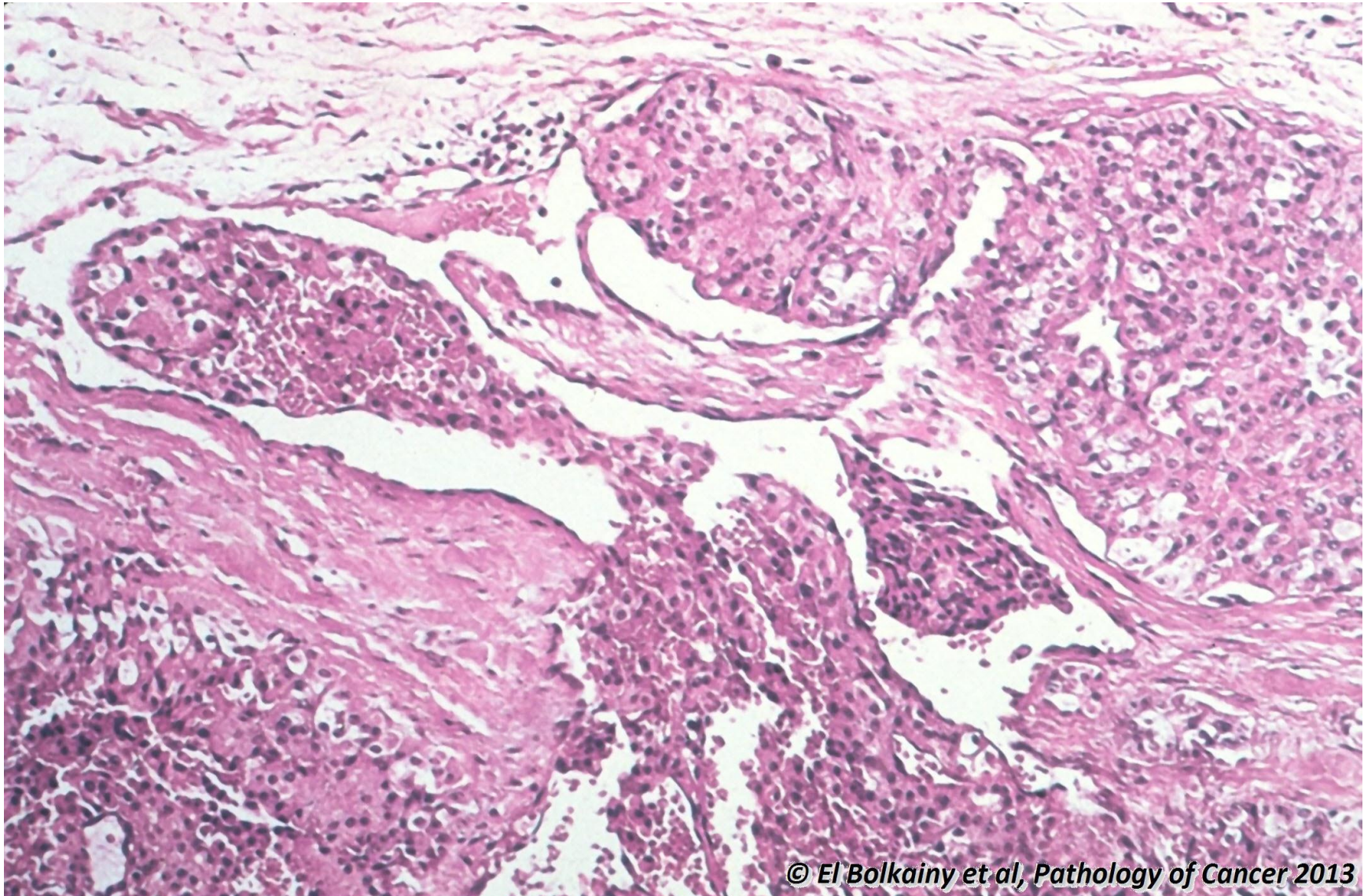
19.13 Follicular carcinoma, angioinvasion of the internal jugular vein.



© El Bolkainy et al, Pathology of Cancer 2013

Picture 19-13 Follicular carcinoma, angioinvasion of the internal jugular vein. The intravascular tumor thrombus is attached to vessel wall and partly covered by endothelium. **A** Gross picture. **B** Histology.

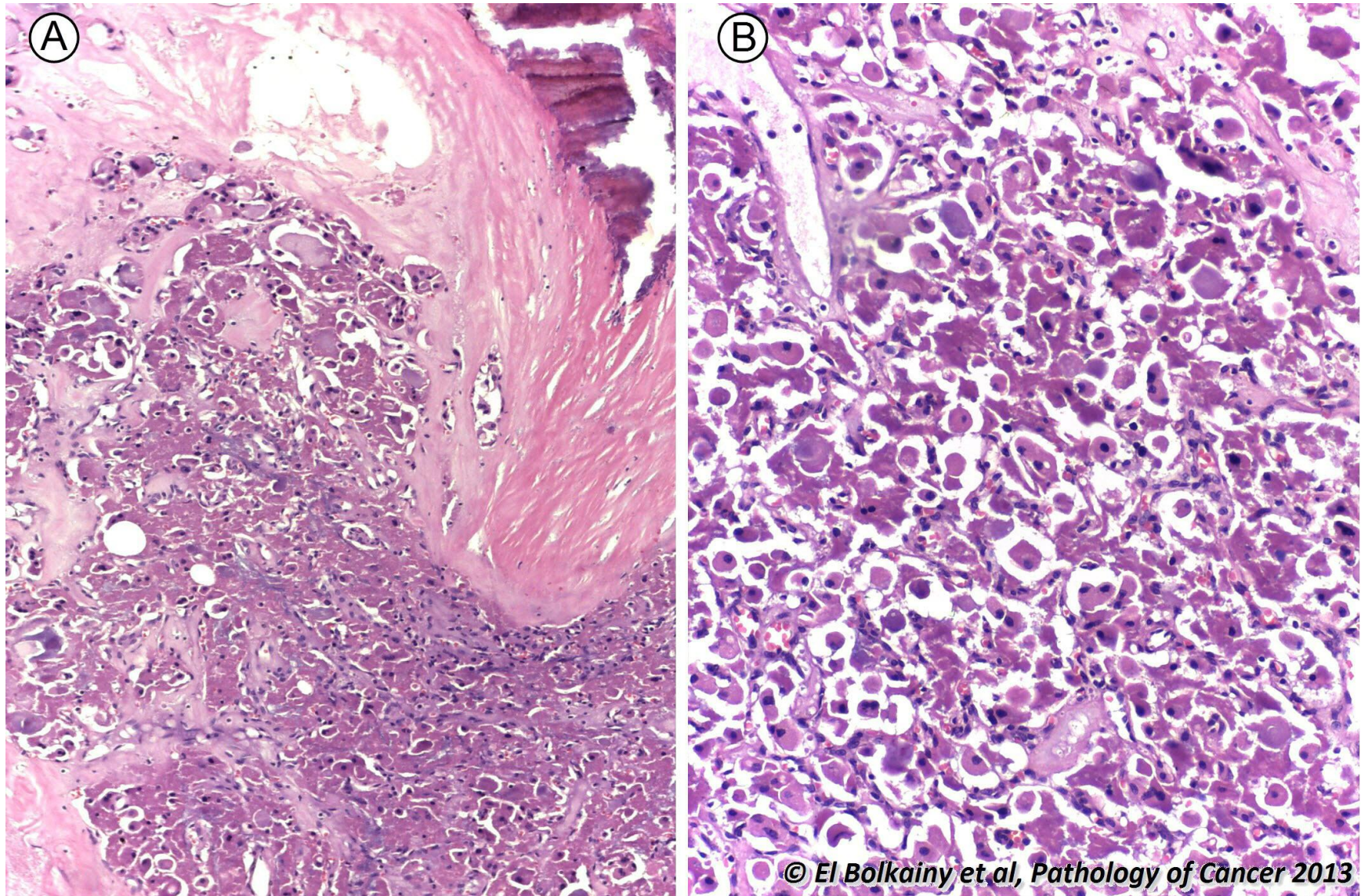
19.14 Follicular carcinoma, histology of angioinvasion.



© El Bolkainy et al, Pathology of Cancer 2013

Picture 19-14 Follicular carcinoma, histology of angioinvasion. Multiple malignant thrombi are present in the thin-walled vessels of tumor capsule.

19.15 Hurthle cell (oncocytic) carcinoma, histology.

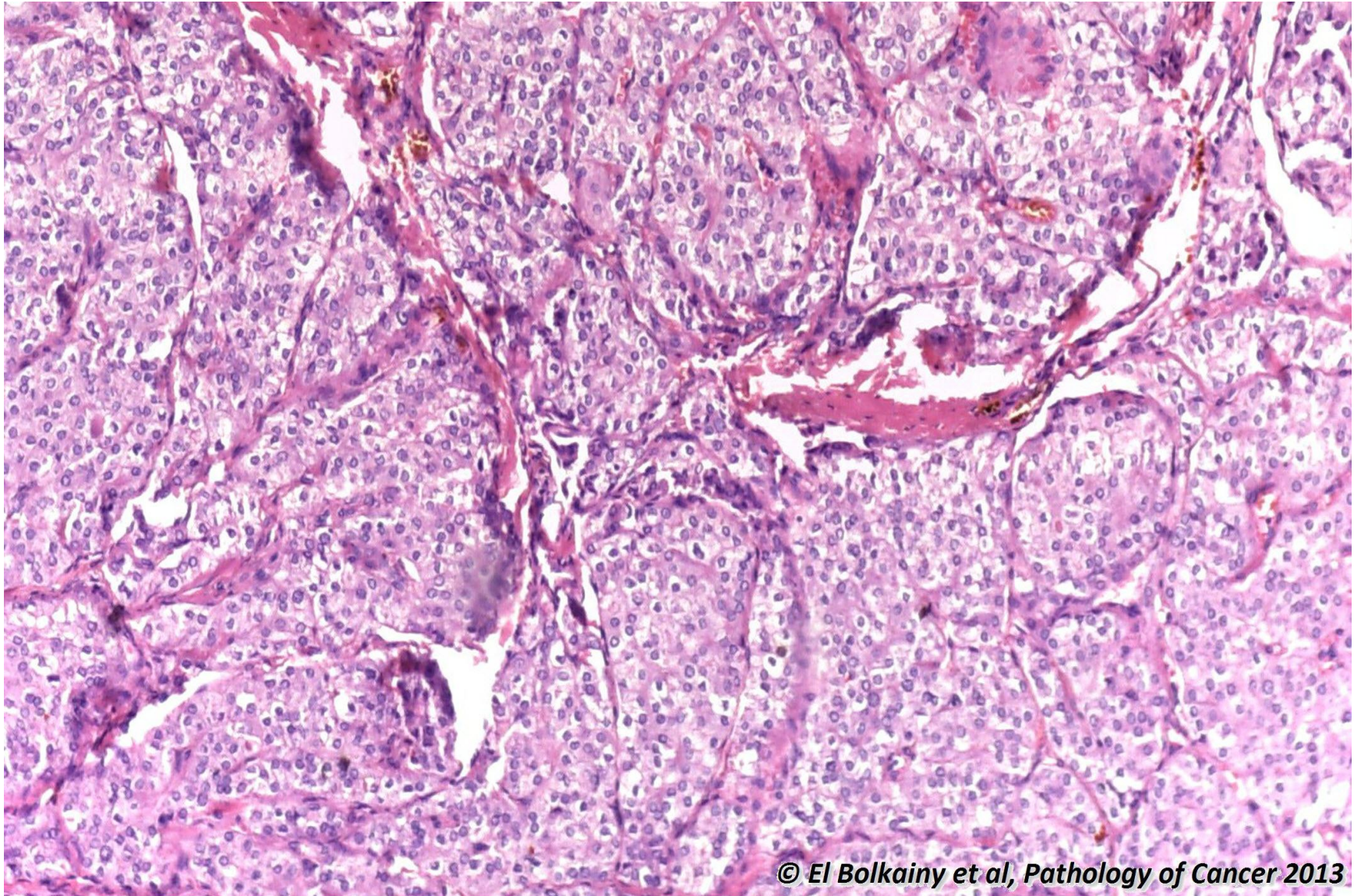


Picture 19-15

Hurthle cell (oncocytic) carcinoma, histology. Carcinoma cells have abundant eosinophilic (red) cytoplasm. The presence of capsular or angioinvasion at capsule differentiates it from hurthe cell adenoma. **A** Low power. **B** High power.

© El Bolkainy et al, Pathology of Cancer 2013

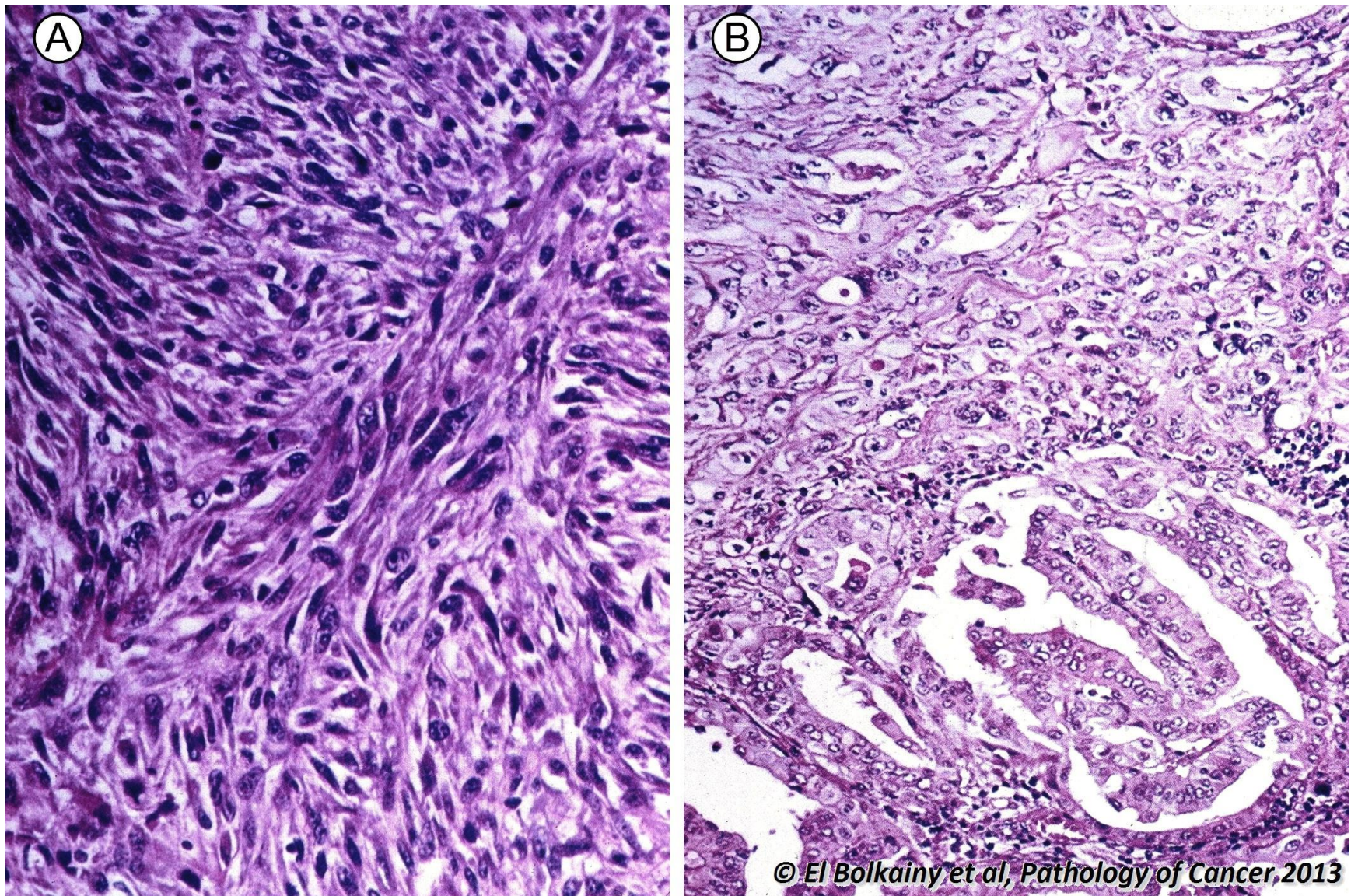
19.16 Insular pattern (insula= islands) of follicular carcinoma, histology.



© El Bolkainy et al, Pathology of Cancer 2013

Picture 19-16 Insular pattern (insula= islands) of follicular carcinoma, histology. The tumor is composed of solid cell groups separated by fibrovascular stroma.

19.17 Undifferentiated (anaplastic) carcinoma, histology.

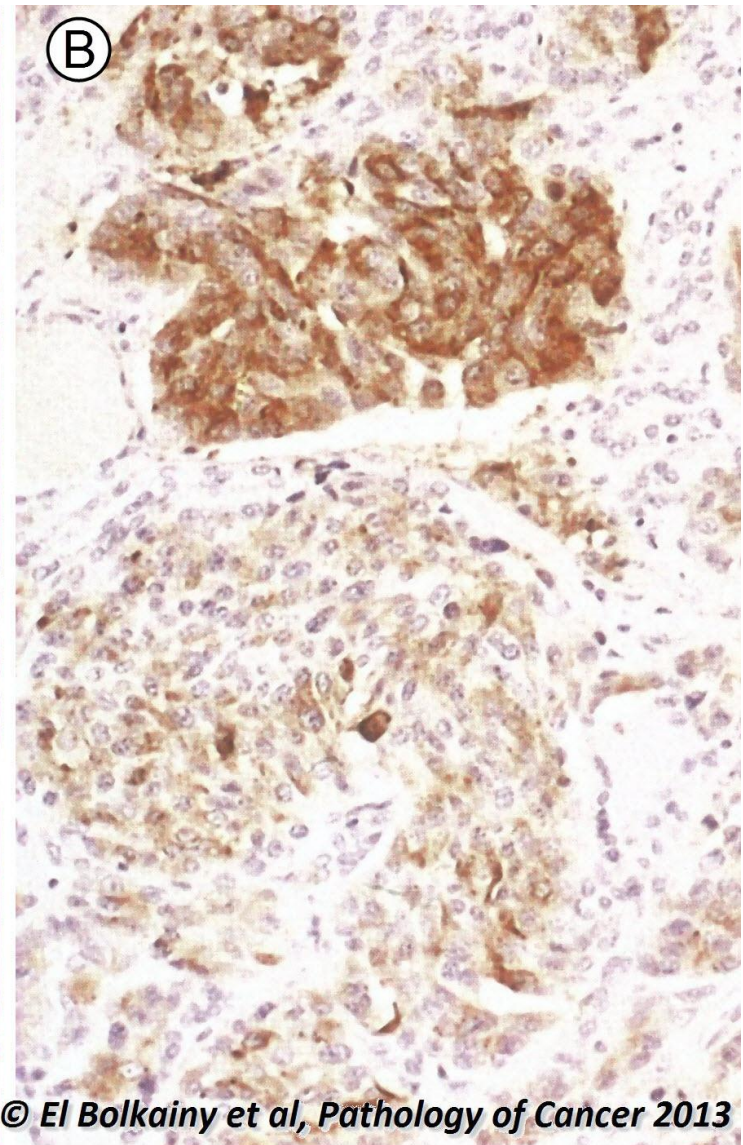
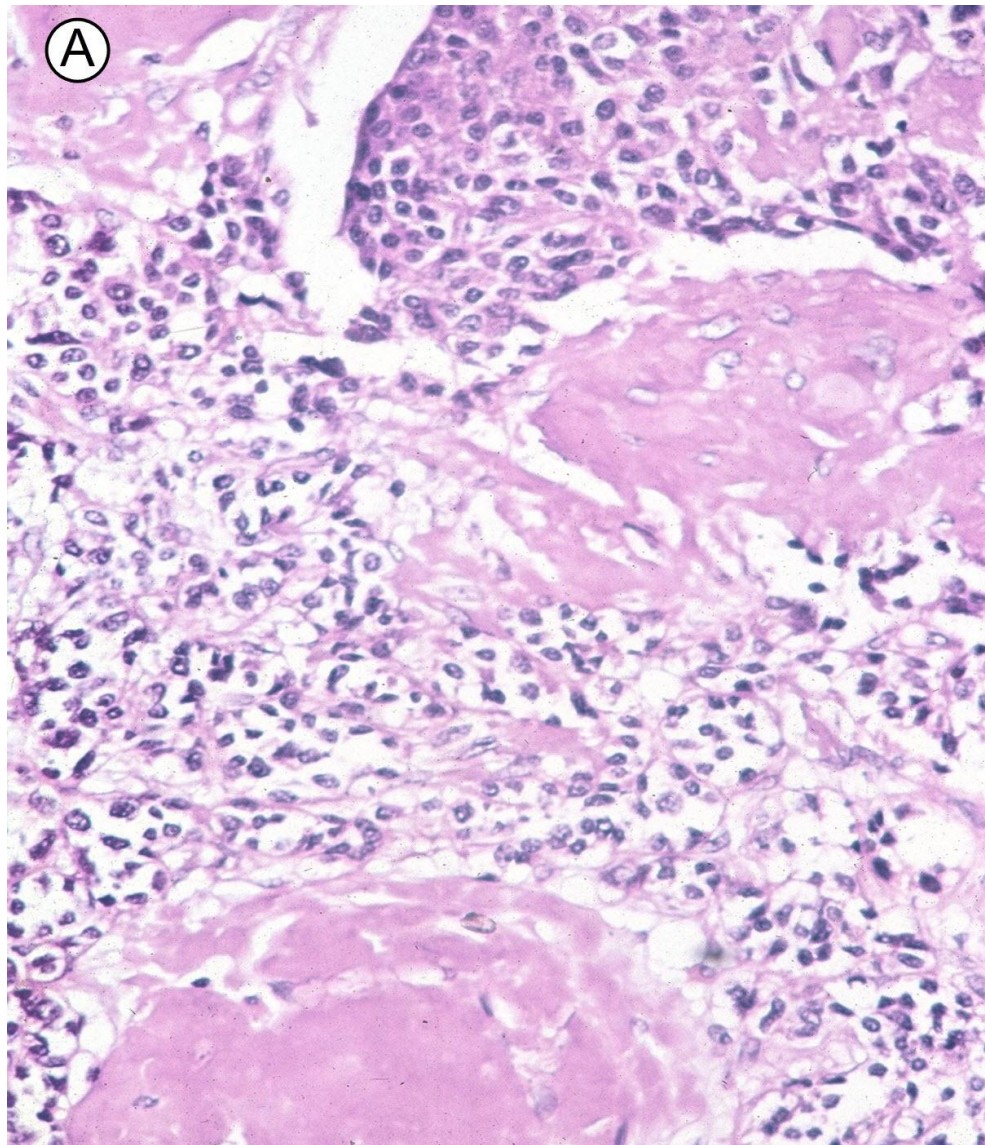


© El Bolkainy et al, Pathology of Cancer, 2013

Picture 19-17

Undifferentiated (anaplastic) carcinoma, histology. **A** This highly aggressive carcinoma is composed of spindle, giant and squamous cells with marked anaplasia and mitosis. **B** Undifferentiated carcinoma developing on top of papillary carcinoma (dedifferentiation phenomenon).

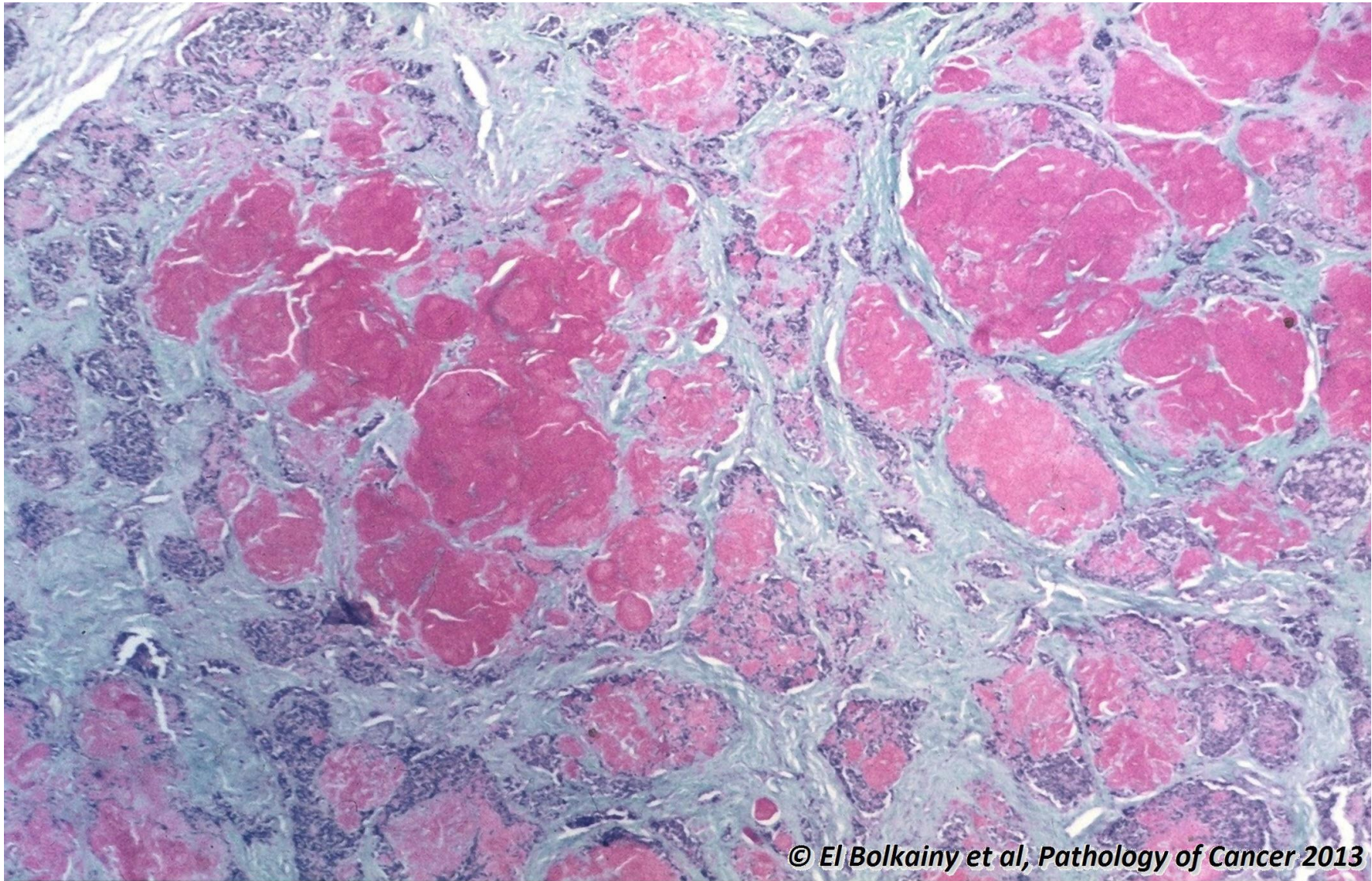
19.18 Medullary carcinoma, histology.



© El Bolkainy et al, Pathology of Cancer 2013

Picture 19-18 Medullary carcinoma, histology. **A** Solid groups of round oval, spindle or plasmacytoid (neuroendocrine c-cell in origin confirmed by chromogranin and calcitonin) in fibrous stroma. **B** Amyloid is evident in stroma in 80% of cases.

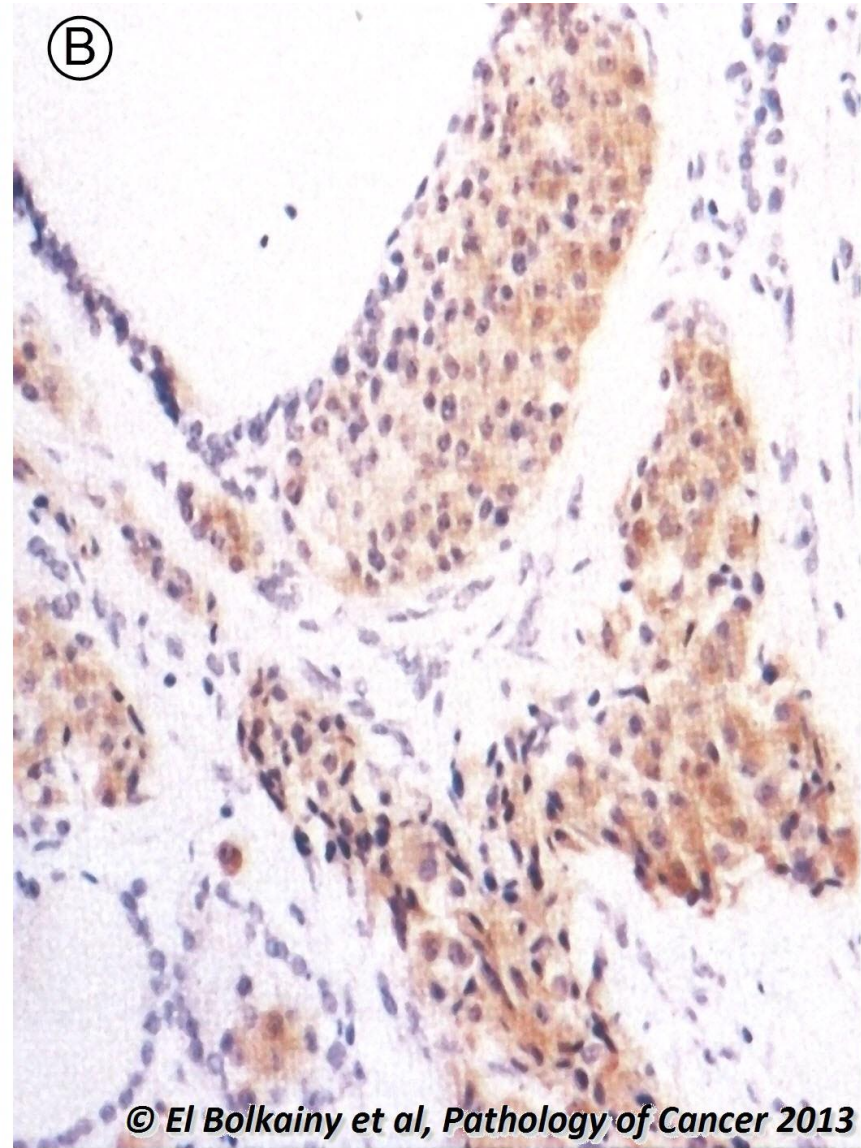
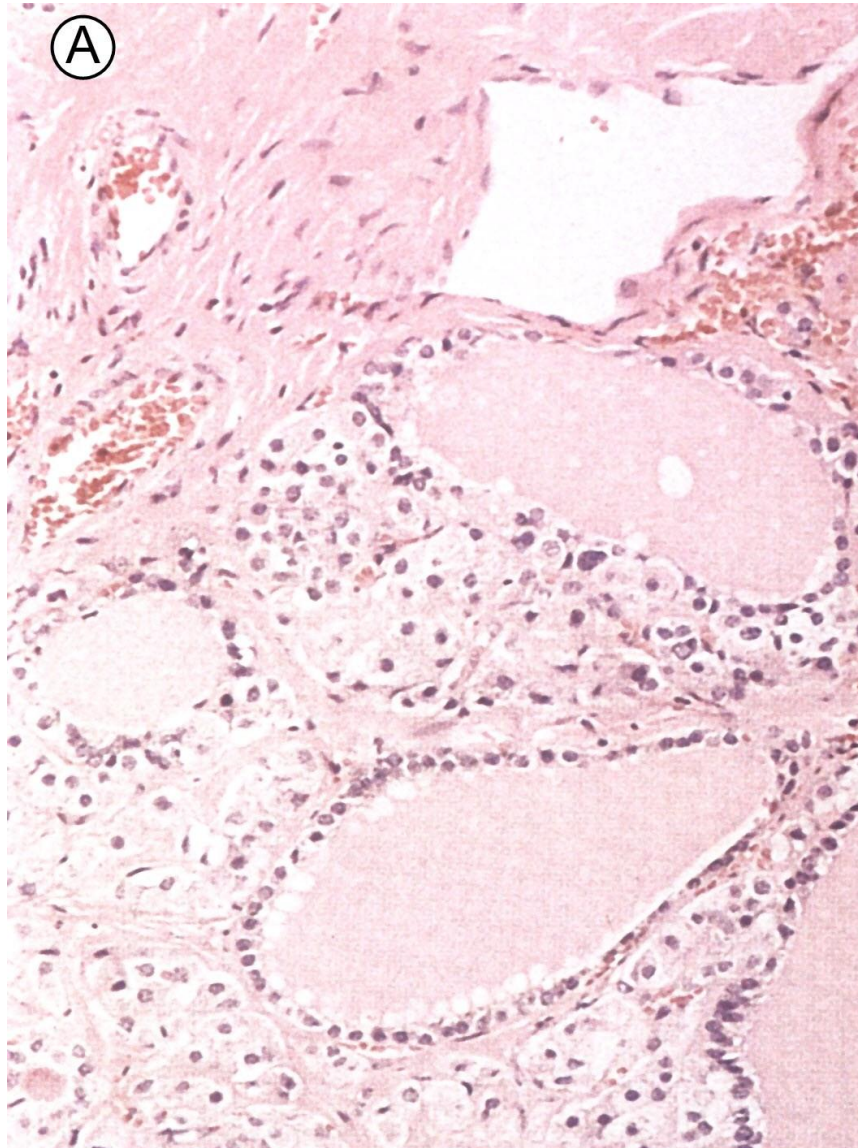
19.19 Medullary carcinoma, histochemistry.



© El Bolkainy et al, Pathology of Cancer 2013

Picture 19-19 Medullary carcinoma, histochemistry. The amyloid in the stroma is positive for congo red (also greenish birefringence in polarized light, not shown).

19.20 C-cell hyperplasia in MEN syndrome.

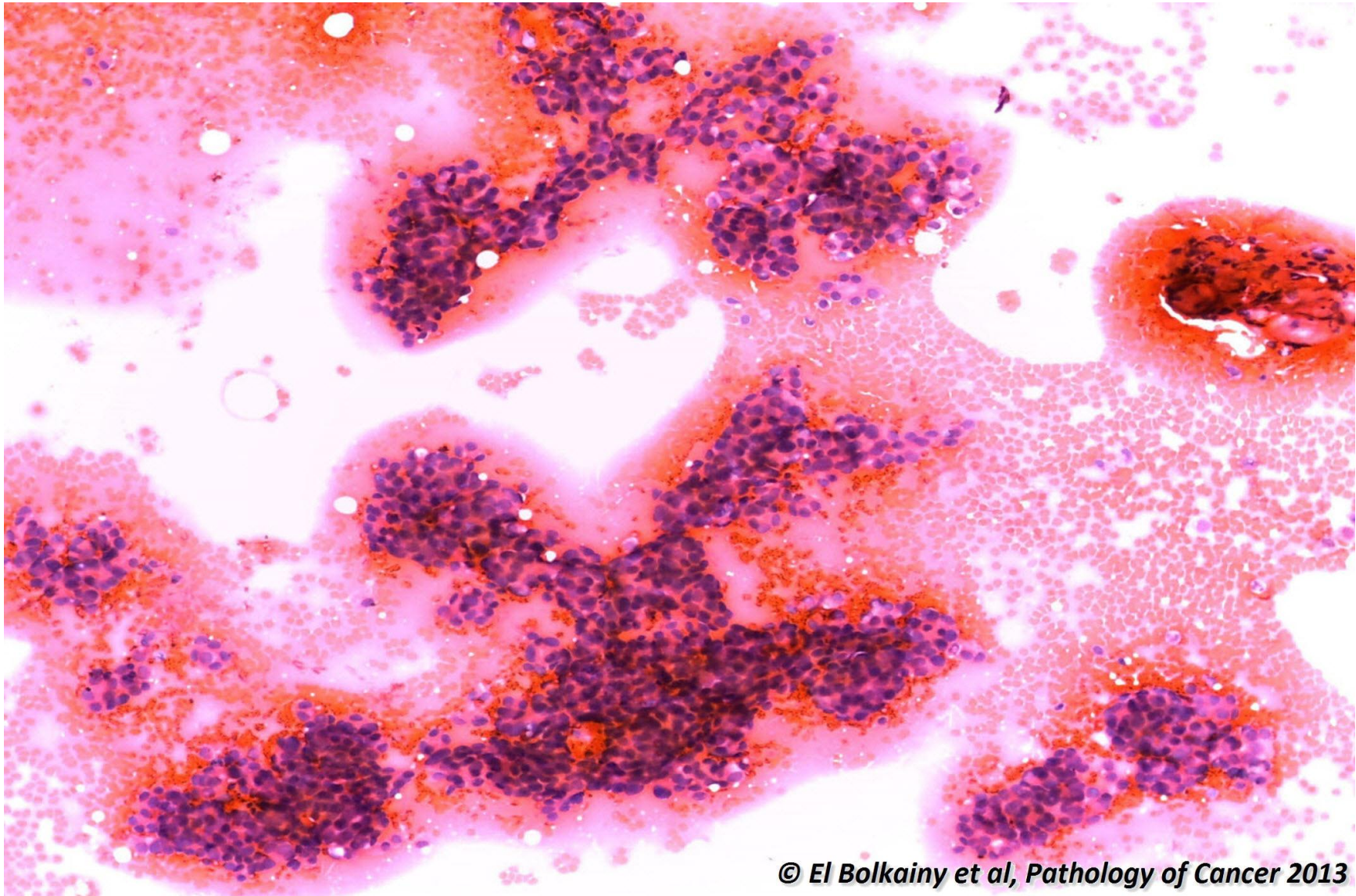


© El Bolkainy et al, Pathology of Cancer 2013

**Picture
19-20**

C-cell hyperplasia in MEN syndrome. This precursor lesion of medullary carcinoma appears as multiple microscopic nests of c- cells (> 50 cells) with bilateral affection of thyroid lobes (tissue samples taken by needle biopsy).

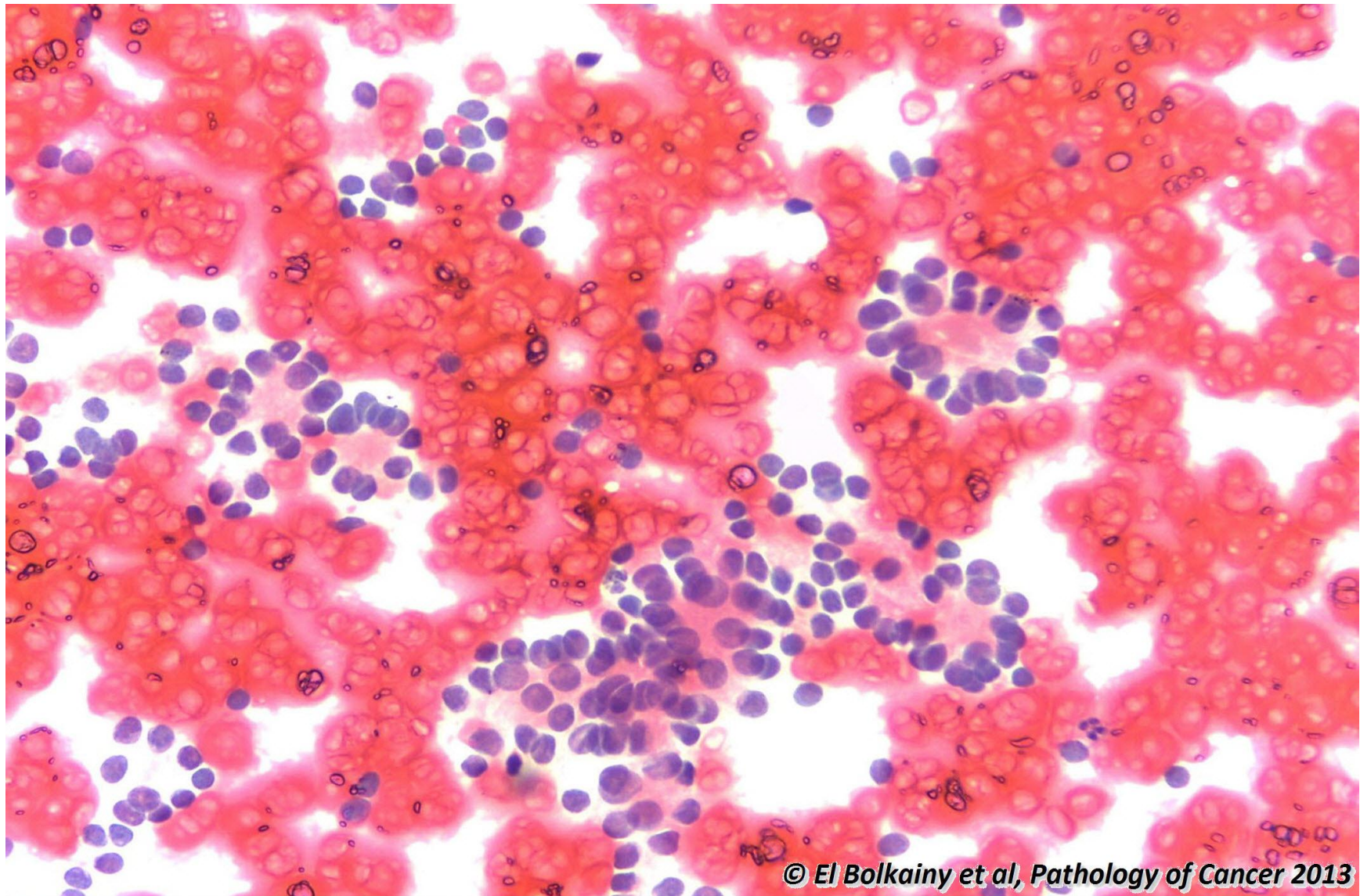
19.21 Papillary carcinoma of thyroid, fine needle aspiration cytology.



© El Bolkainy et al, Pathology of Cancer 2013

Picture 19-21 Papillary carcinoma of thyroid, fine needle aspiration cytology. A branching papillary cell cluster is observed with crowded cells lacking colloid. The nuclei may show grooves and appear pale due to cytoplasmic inclusions. Psammoma bodies may be seen.

19.22 Follicular lesions of thyroid, fine needle aspiration cytology.

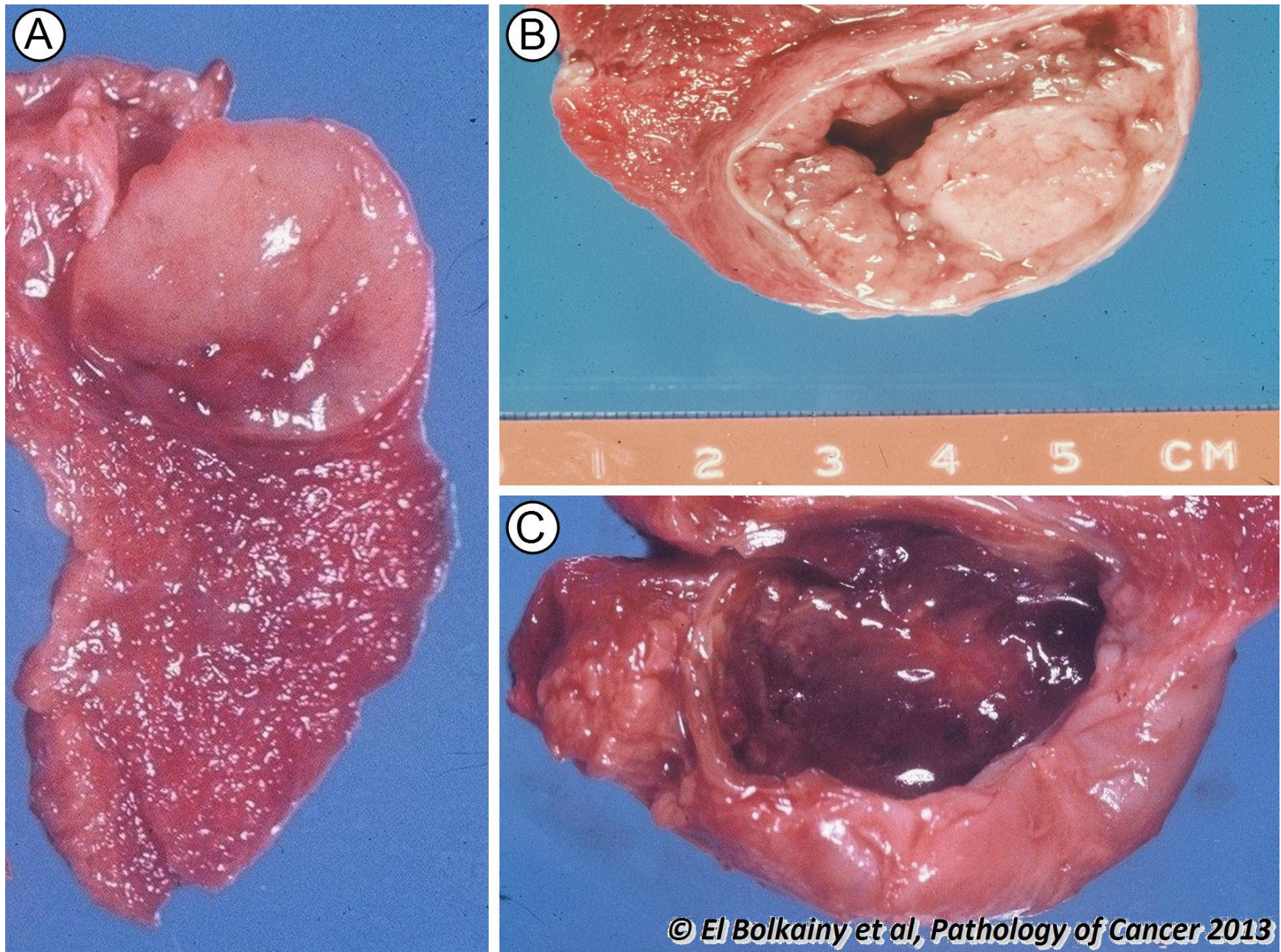


© El Bolkainy et al, Pathology of Cancer 2013

Picture
19-22

Follicular lesions of thyroid, fine needle aspiration cytology. Follicular epithelium is radially arranged around colloid. This pattern is not diagnostic, since it may be observed in hyperplasia, adenoma and carcinoma. Surgical excision is needed to establish the exact diagnosis.

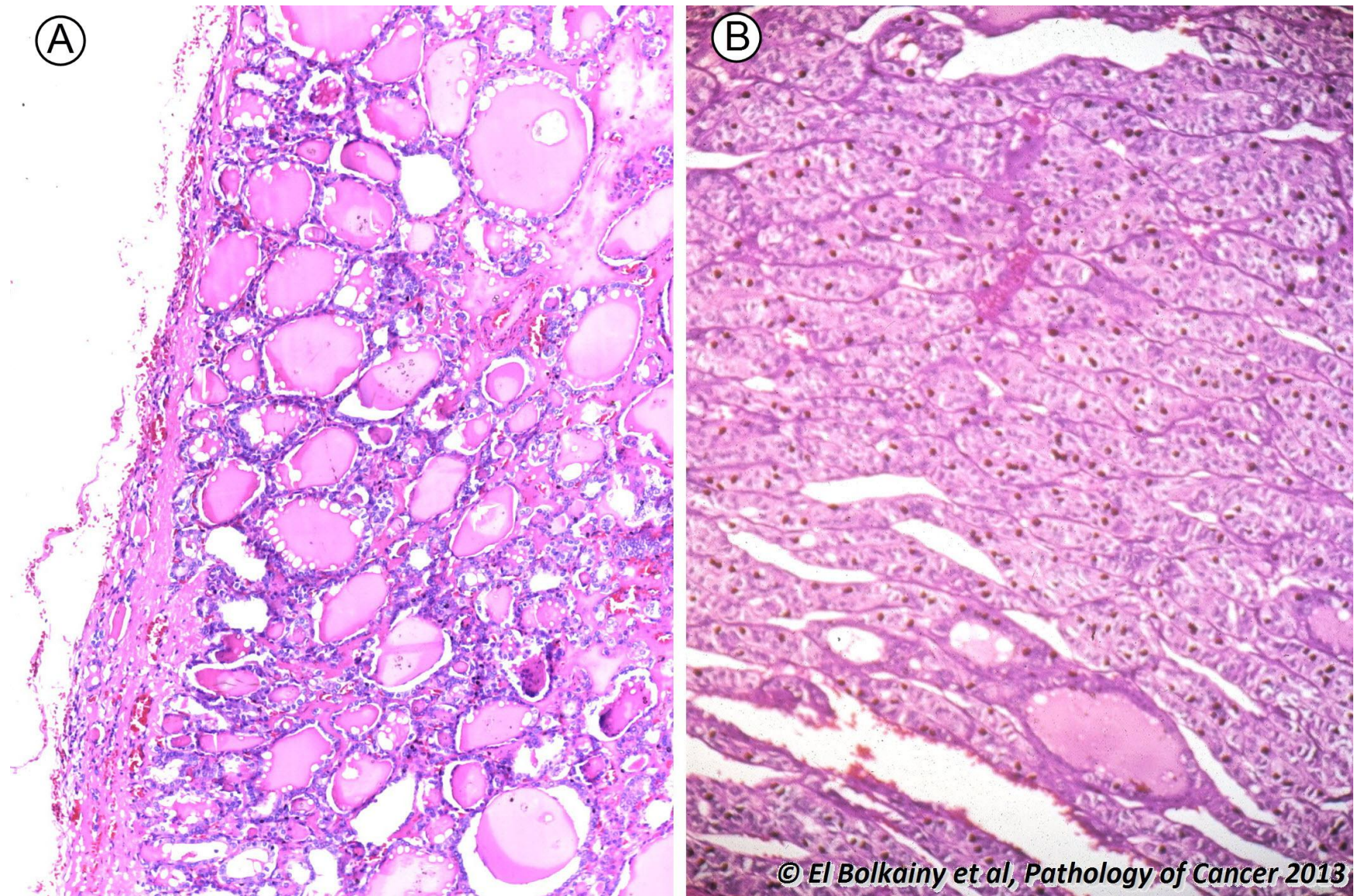
19.23 Follicular adenoma, gross features.



Picture 19-23 Follicular adenoma, gross features. **A** Well encapsulated gray brown glistening cut section. **B** Cystic change in adenoma (cystadenoma). **C** Hemorrhage in an adenoma.

© El Bolkainy et al, Pathology of Cancer 2013

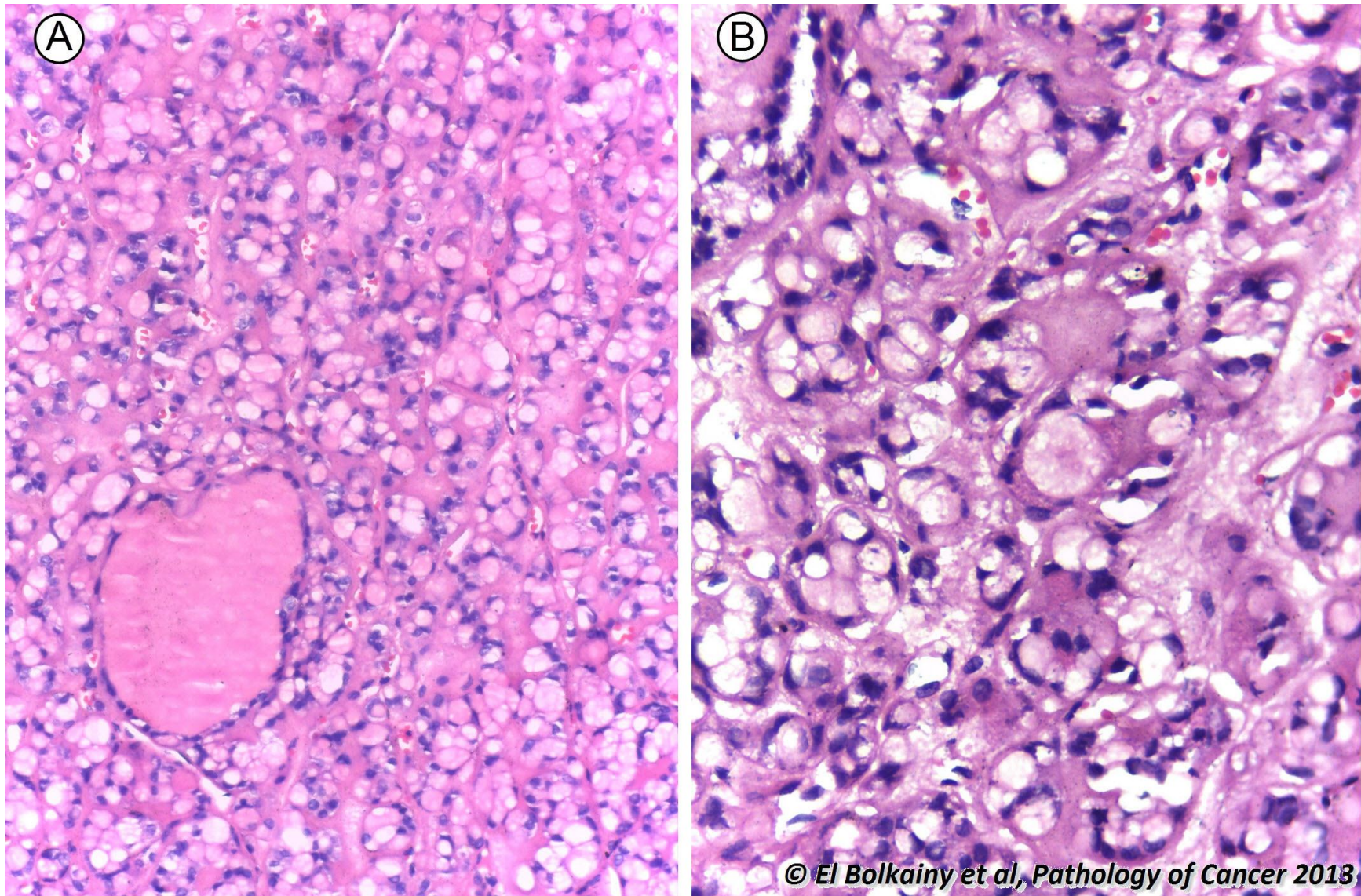
19.24 Follicular adenoma, histology.



Picture 19-24 Follicular adenoma, histology. **A** Follicular pattern: rounded microfollicles lined by a monolayered uniform cells. **B** Trabecular pattern, covered by thin intact capsule containing well muscularized blood vessels.

© El Bolkainy et al, Pathology of Cancer 2013

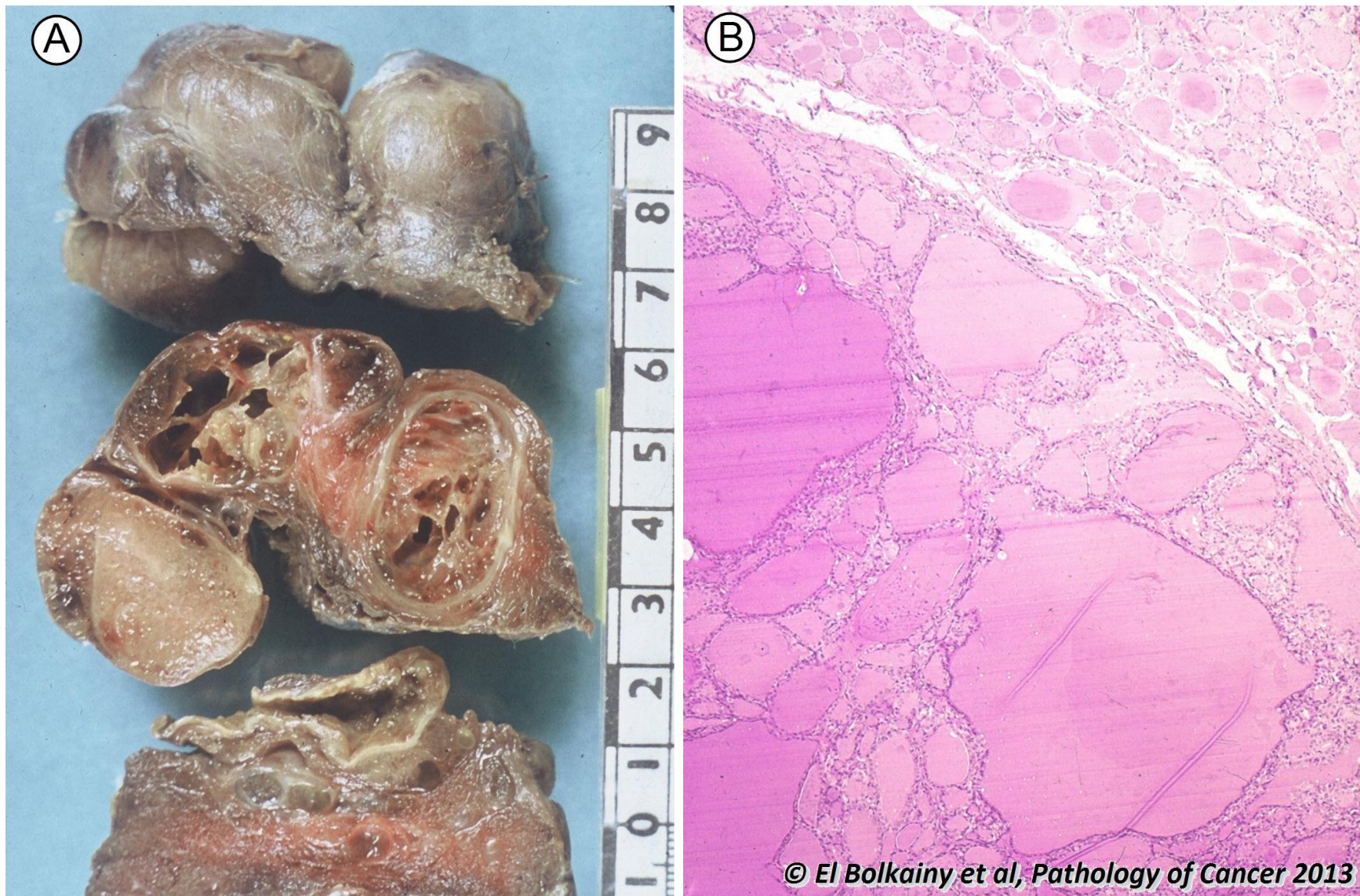
19.25 Follicular adenoma, histology of signet ring variant.



Picture 19-25

Follicular adenoma, histology of signet ring variant. In this rare benign tumor, cytoplasmic vacuoles are present in epithelium (positive for thyroglobulin) and displacing the nucleus. This should not be misdiagnosed as metastatic signet ring adenocarcinoma. **A** Low power. **B** High power.

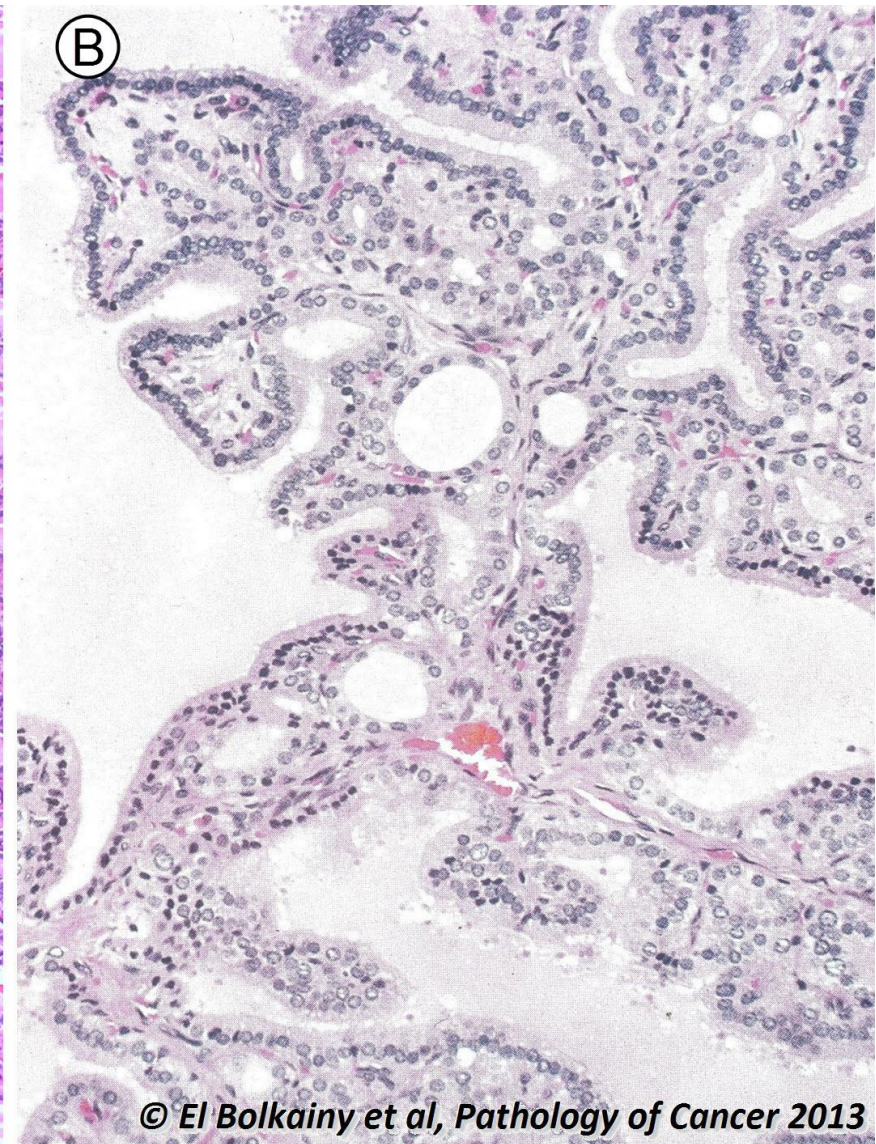
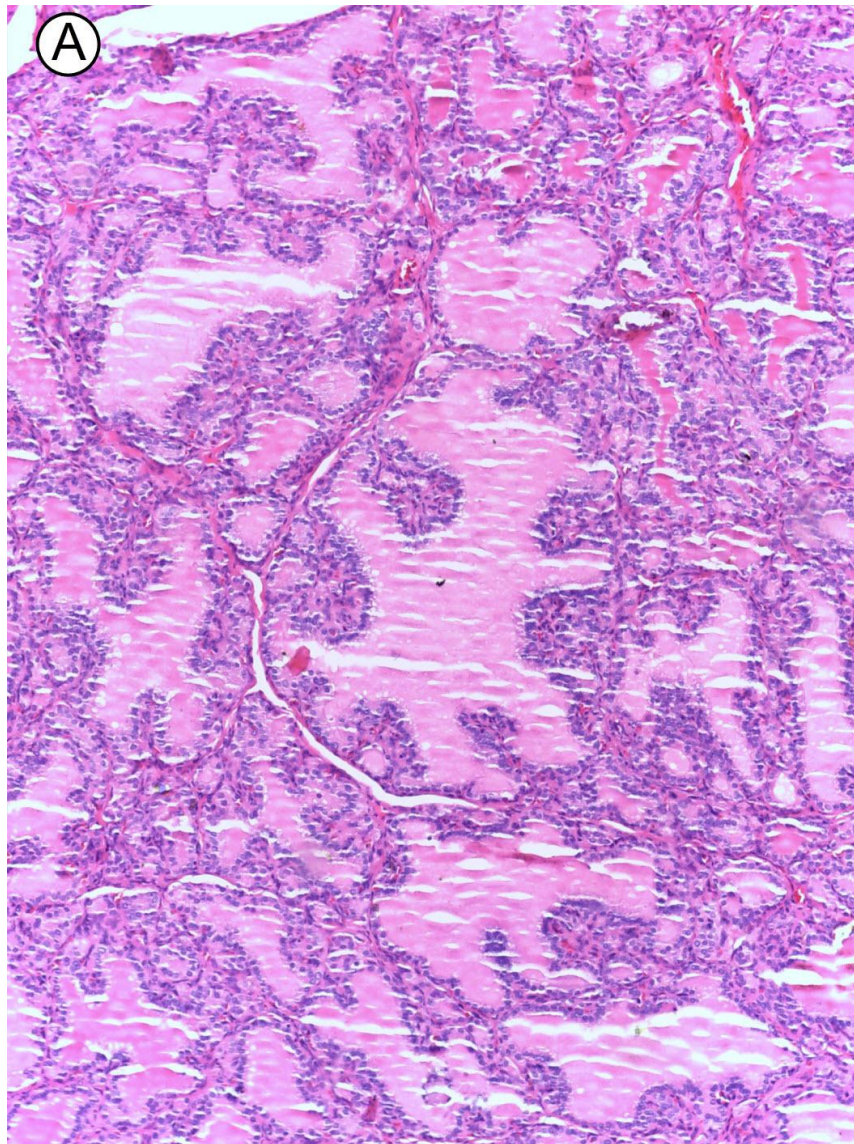
19.26 Nodular hyperplasia of thyroid.



**Picture
19-26**

Nodular hyperplasia of thyroid. A Gross appearance: multinodular, brownish shining appearance (colloid) separated by thin stroma. B Histology composed mainly of large follicles and lack a definite capsule, but, pseudocapsule of compressed thyroid tissue.

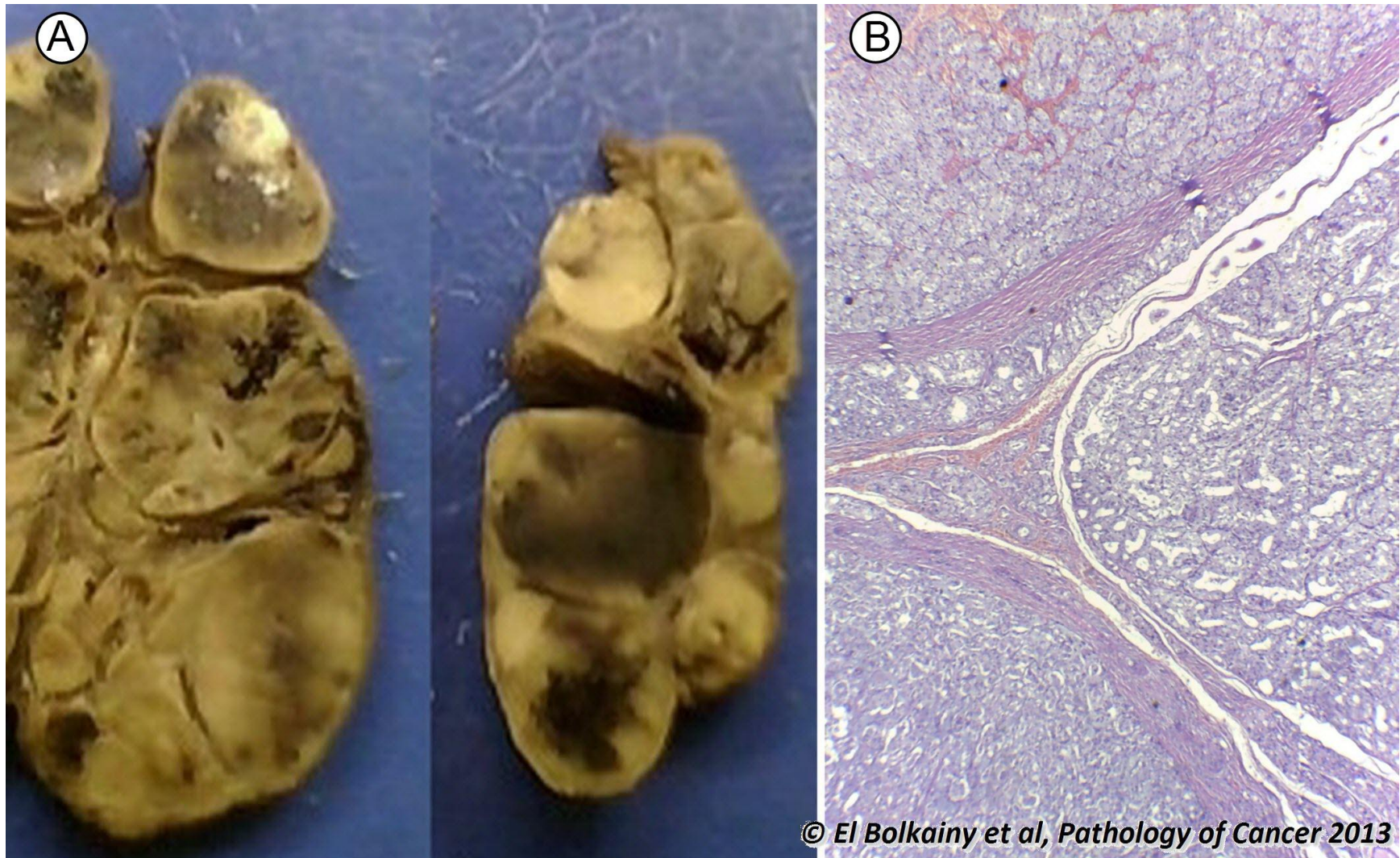
19.27 Nodular hyperplasia, histology of pseudopapillary pattern.



© El Bolkainy et al, Pathology of Cancer 2013

Picture 19-27 Nodular hyperplasia, histology of pseudopapillary pattern. **A** Short epithelial folds into dilated follicles. **B** Pseudopapillary pattern contain thyroid follicles in the stroma and covered by hyperchromatic (non-clear) nuclei.

19.28 Dyshormonogenetic goiter.

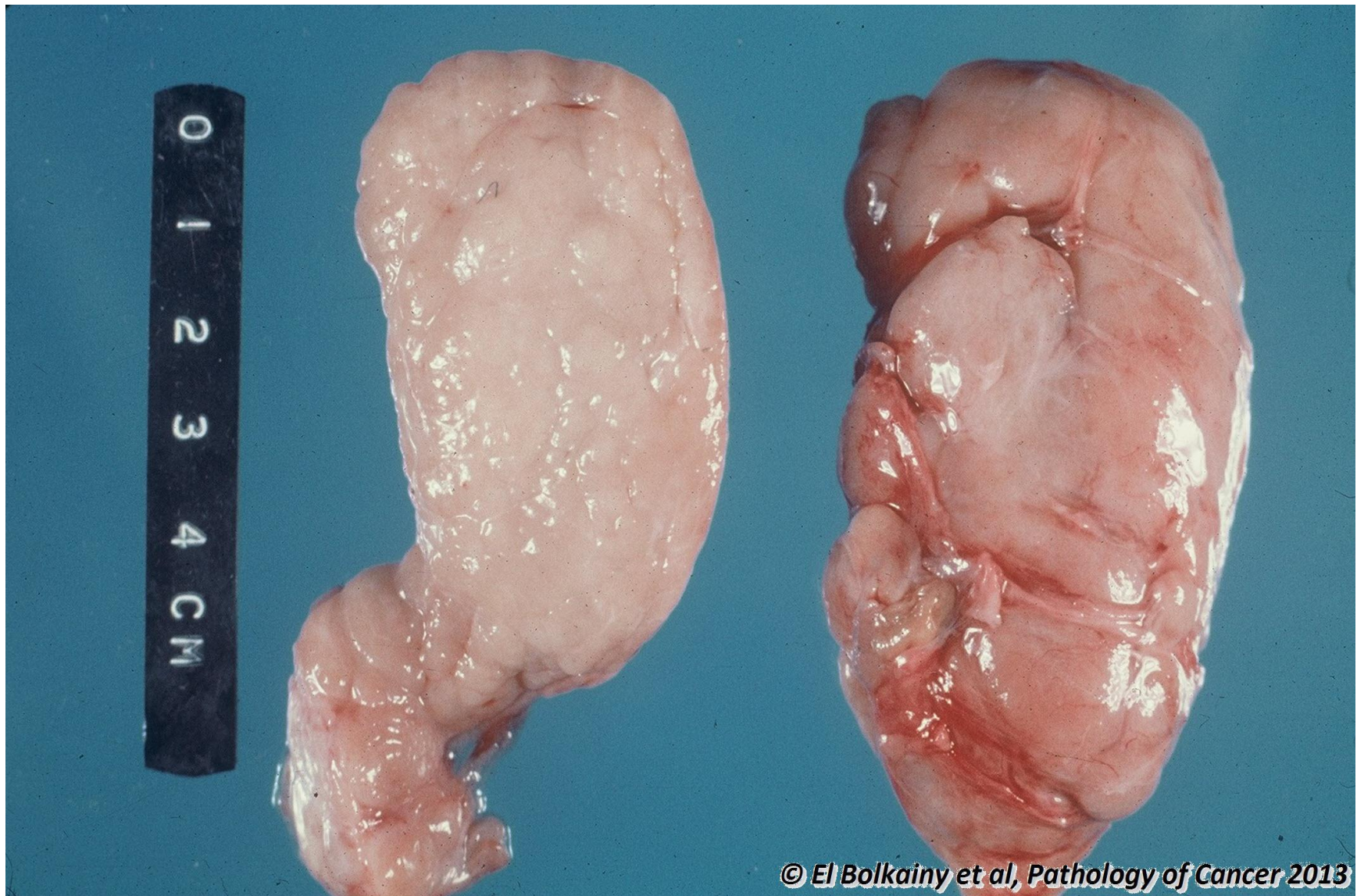


© El Bolkainy et al, Pathology of Cancer 2013

**Picture
19-28**

Dyshormonogenetic goiter. This pediatric disease results from an inherited defect in thyroid hormone synthesis resulting in hypothyroidism and thyroid hyperplasia. **A** Grossly: multiple nodules of variable size separated by dense stroma. **B** Histology: microfollicles lacking colloid, solid areas, and atypical pleomorphic cells (seen only in parenchyma between nodules).

19.29 Chronic lymphocytic thyroiditis (Hashimoto's disease).

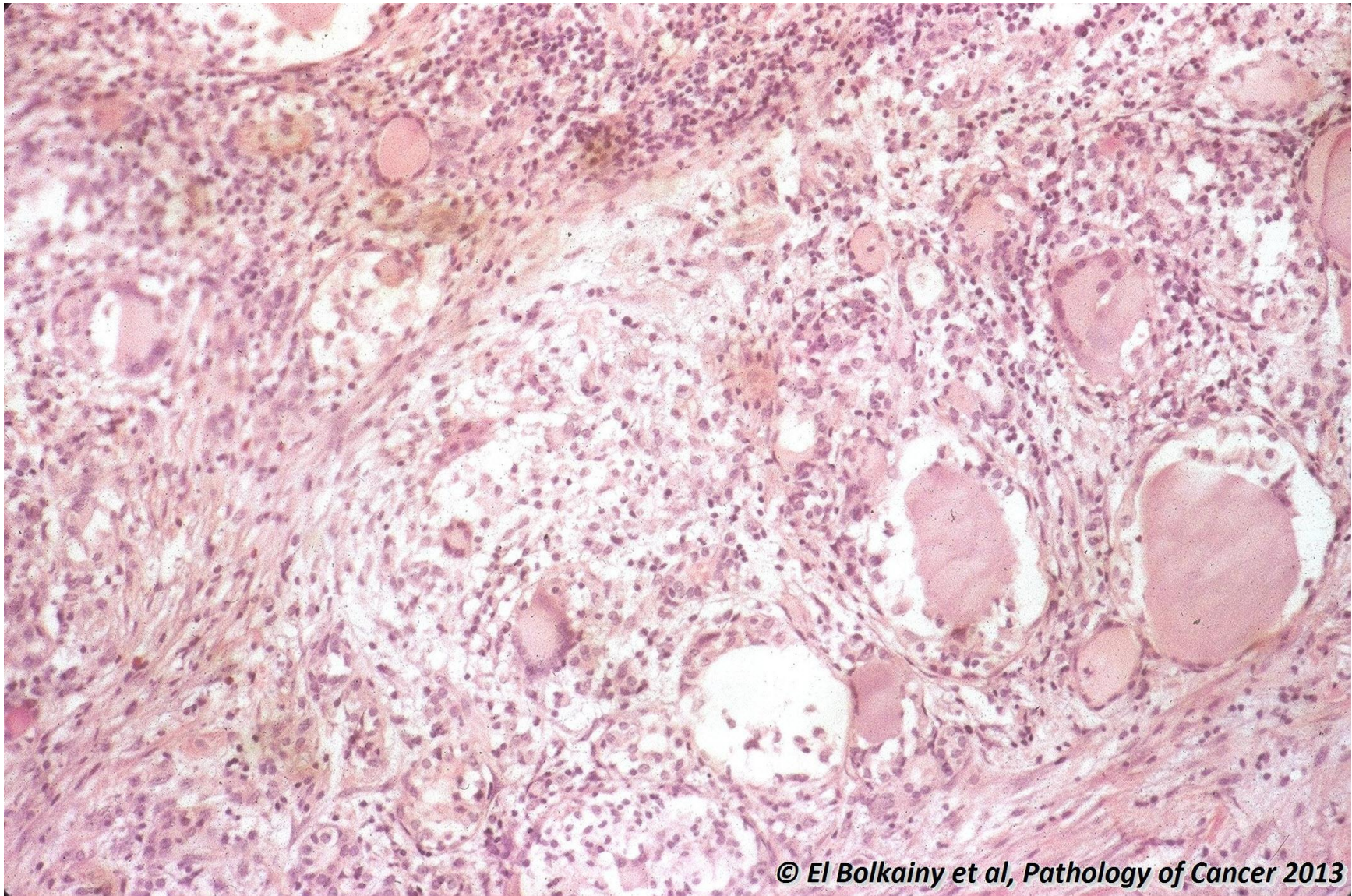


© El Bolkainy et al, Pathology of Cancer 2013

**Picture
19-29**

Chronic lymphocytic thyroiditis (Hashimoto's disease). This is an autoimmune disease of adults, associated with hypothyroidism and increased risk of lymphoma. Grossly, the thyroid is slightly enlarged but keeping its shape and cut section whitish in color. The histology is characterized by oxiphilic cytoplasm and stroma rich in lymphoid tissue with germinal centers.

19.30 Granulomatous thyroiditis (de-Quervain disease).



© El Bolkainy et al, Pathology of Cancer 2013

Picture 19-30

Granulomatous thyroiditis (de-Quervain disease). This represents a reaction to virus infection affecting adults. Histologically, there is focal destruction of follicles with exudate of lymphocytes, histiocytes and foreign body giant cells.

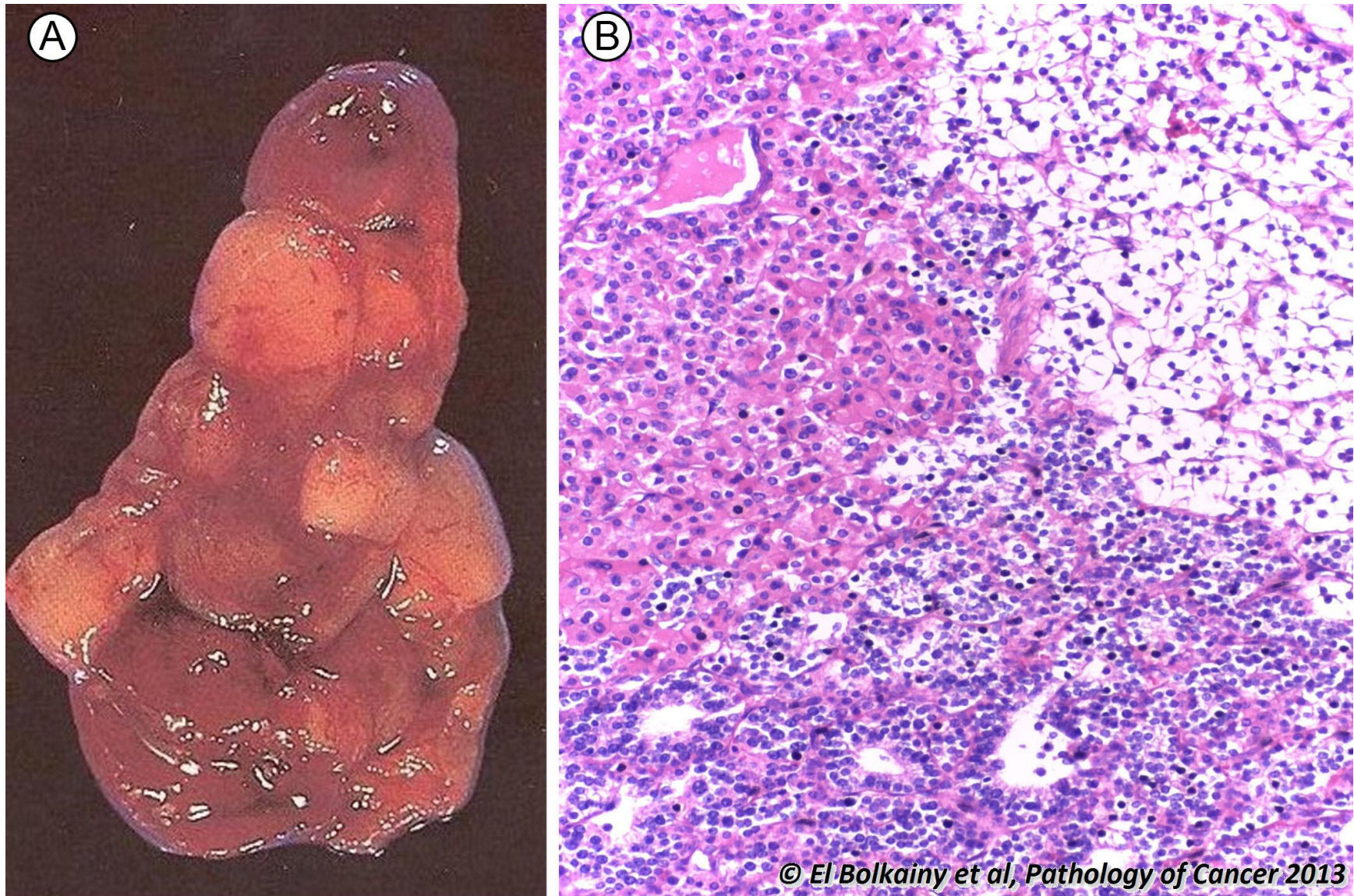
19.31 Thyroid teratoma, gross features.



Picture
19-31

Thyroid teratoma, gross features. The mass is composed of multilocular cysts, solid and bony parts. The histology is complex, containing representative tissues of the three germ layers. Thyroid teratoma is benign in infants, but, malignant in adult patients.

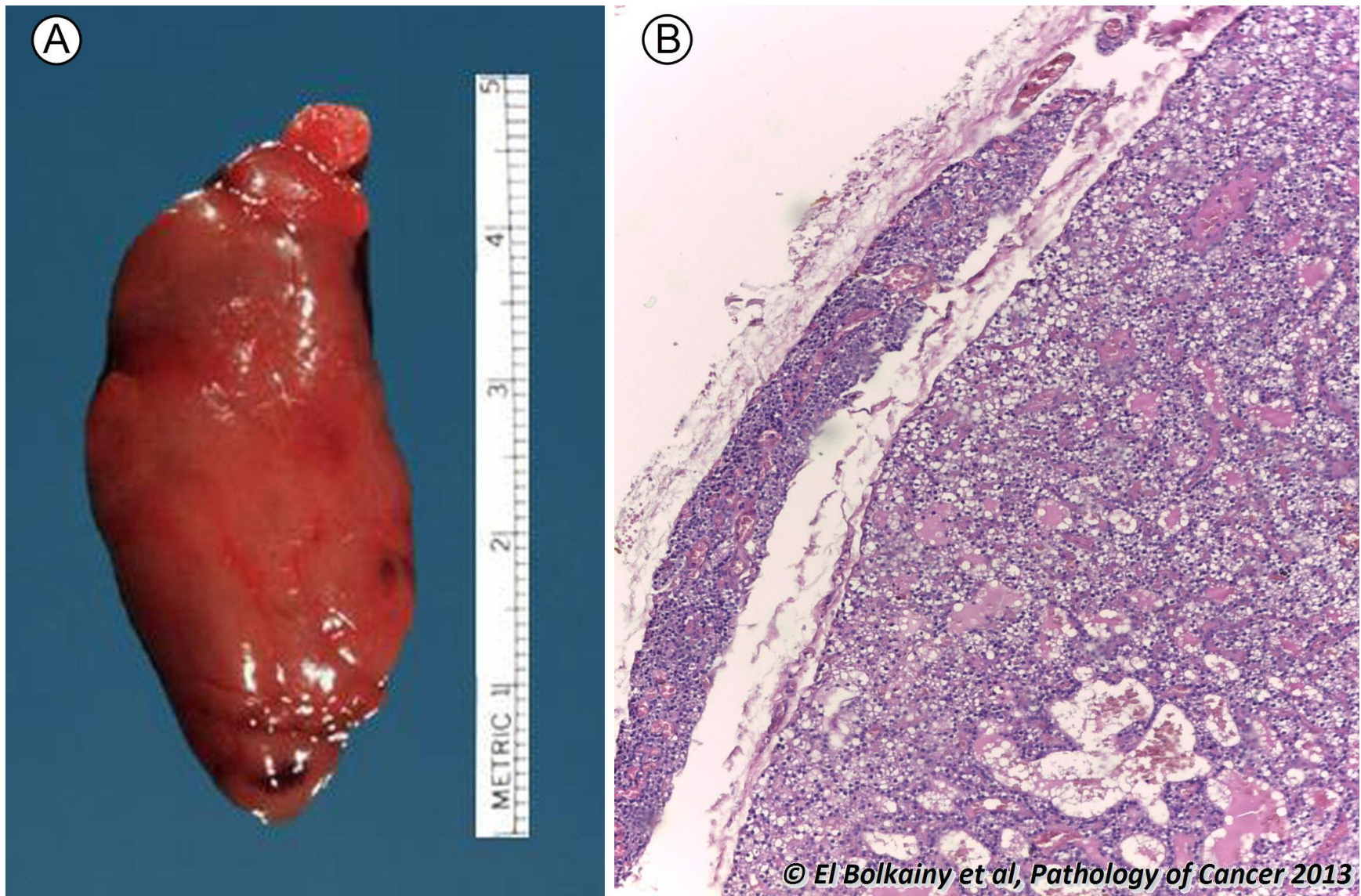
19.32 Parathyroid hyperplasia.



Picture 19-32

Parathyroid hyperplasia. **A** Gross features: All glands are affected, diffuse or nodular enlargement. **B** Histologically, there is hypercellularity with increase of chief and oxyphil cells associated with decrease of intraglandular fat. Hyperplasia is the cause of 15% of cases of hyperparathyroidism.

19.33 Parathyroid adenoma.

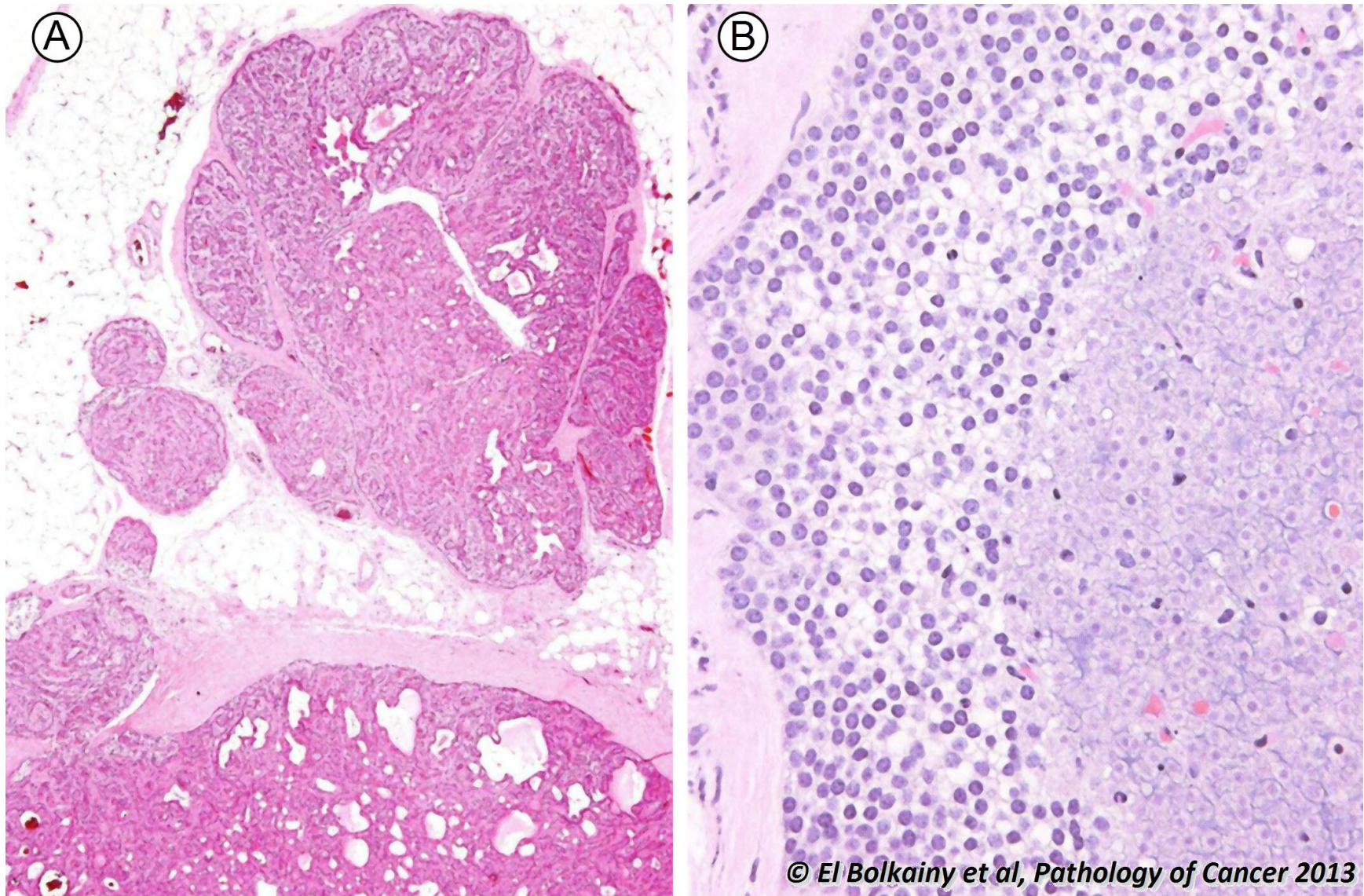


Picture 19-33

Parathyroid adenoma. **A** Gross features: single gland affection, nodule with smooth surface. **B** Histologically, it is composed of either chief or oxyphil cells, compressing normal parathyroid gland near the capsule. It accounts for about 80% of hyperparathyroidism.

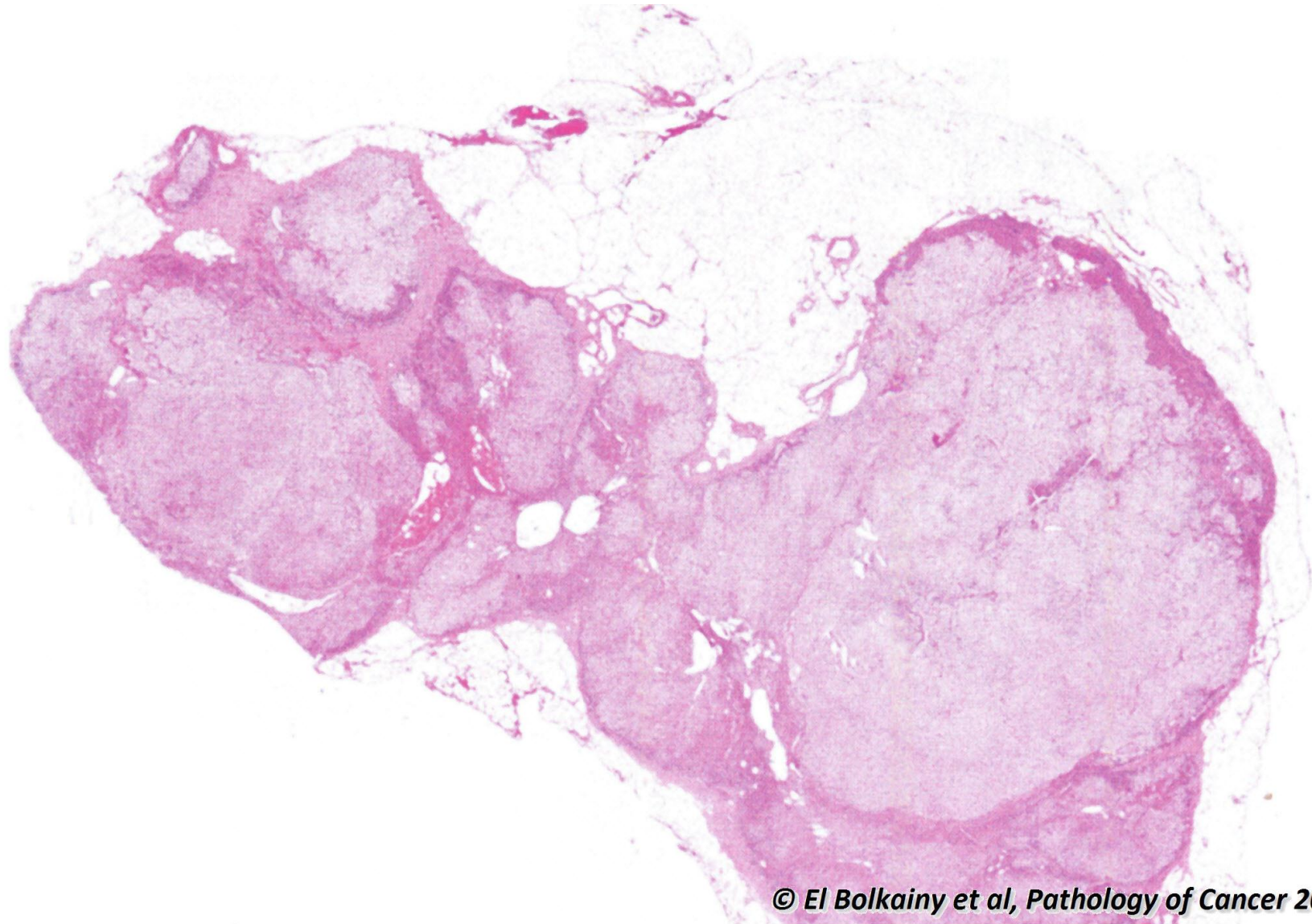
© El Bolkainy et al, Pathology of Cancer 2013

19.34 Parathyroid carcinoma.



Picture 19-34 Parathyroid carcinoma. **A and B** This exceedingly rare neoplasm must be distinguished from the much more common adenoma by the following large palpable mass, marked hypercalcemia, invasion of capsule, thyroid gland, fat, angioinvasion, focal necrosis, KI-67 index > 5 / HPF and abnormal mitosis.

19.35 Adrenal cortical nodular hyperplasia, histology.



© El Bolkainy et al, *Pathology of Cancer 2013*

Picture 19-35 **Adrenal cortical nodular hyperplasia, histology.** This is a common non-functioning incidental finding (3% of elderly population). Histologically, multiple adrenal cortical nodules are evident of variable size (3-10 mm), composed of clear (lipid-rich) adrenal cortical cells.

19.36 Adrenal cortical adenoma, gross features.

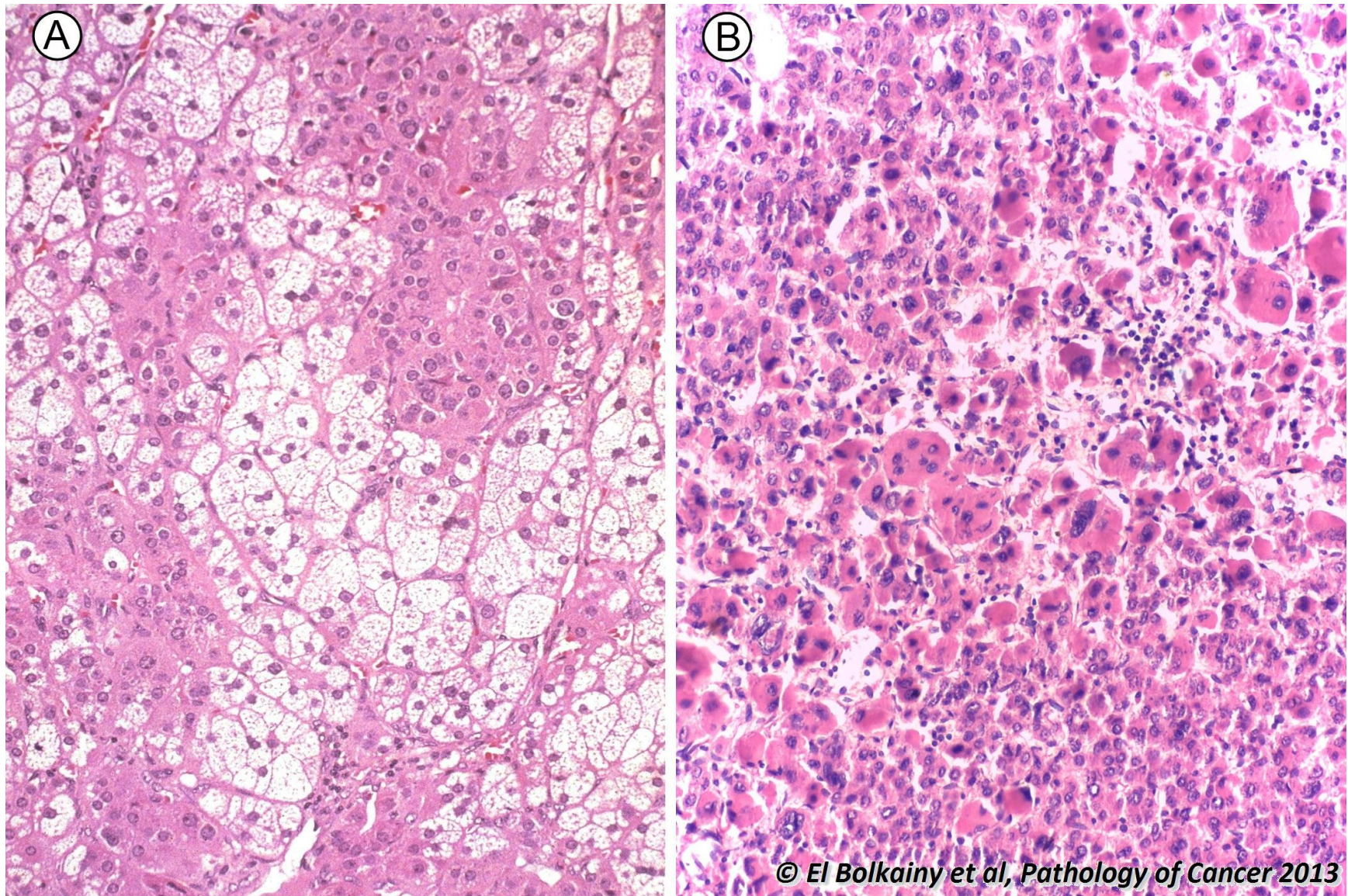


© El Bolkainy et al, Pathology of Cancer 2013

**Picture
19-36**

Adrenal cortical adenoma, gross features. Solitary small tumor (2cm), golden yellow in color and circumscribed.

19.37 Adrenal cortical adenoma, histology.



**Picture
19-37**

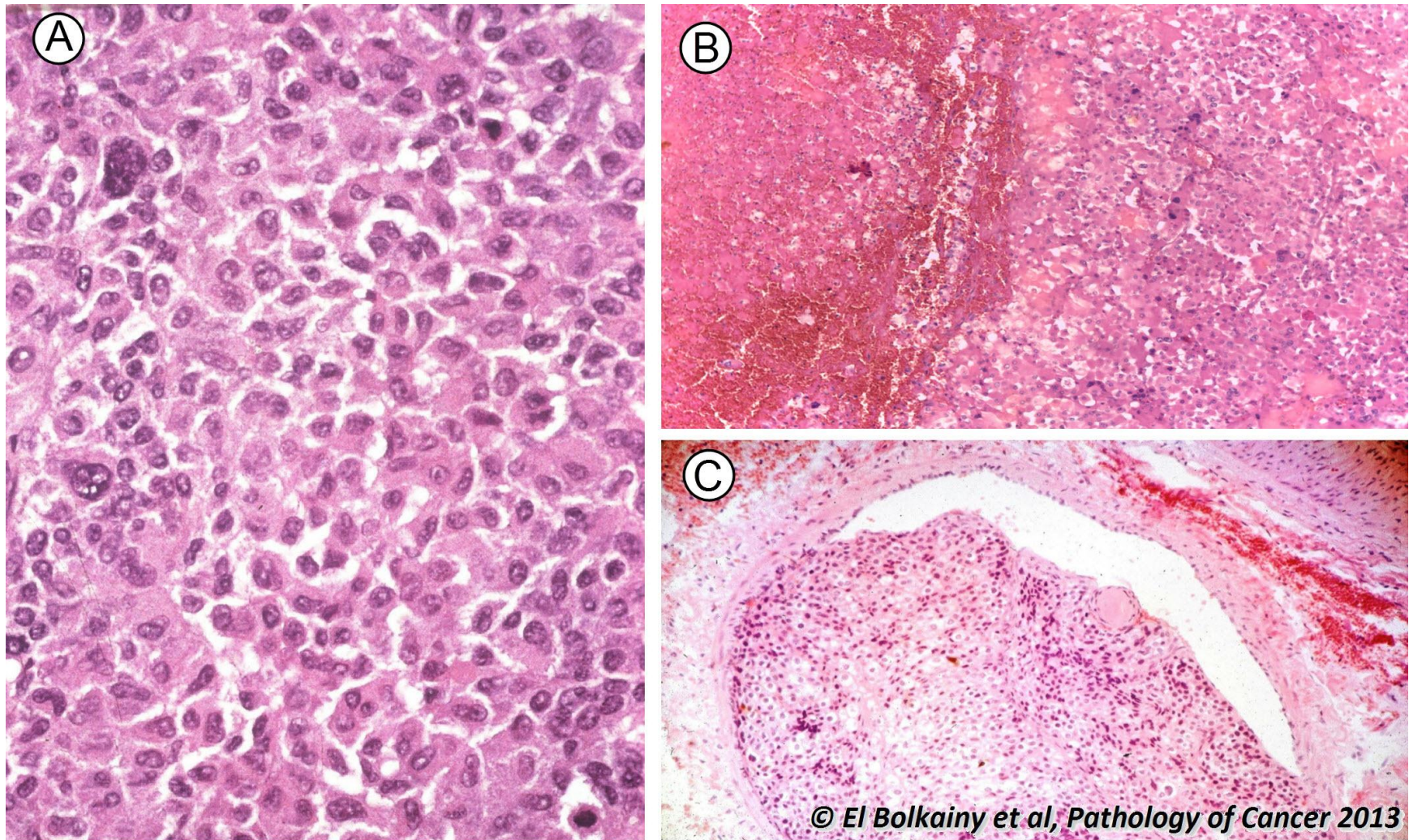
Adrenal cortical adenoma, histology. **A** A mixture of lipid-rich clear cells, as well as, cells with eosinophilic cytoplasm. **B** Pleomorphic hyperchromatic nuclei (symplastic change) in absence of mitosis is not a feature of malignancy, but a result of polyploidy. The tumor is immunoreactive to vimentin, inhibin and Melan-A, but negative for chromogranin.

19.38 Adrenal cortical carcinoma, gross features.



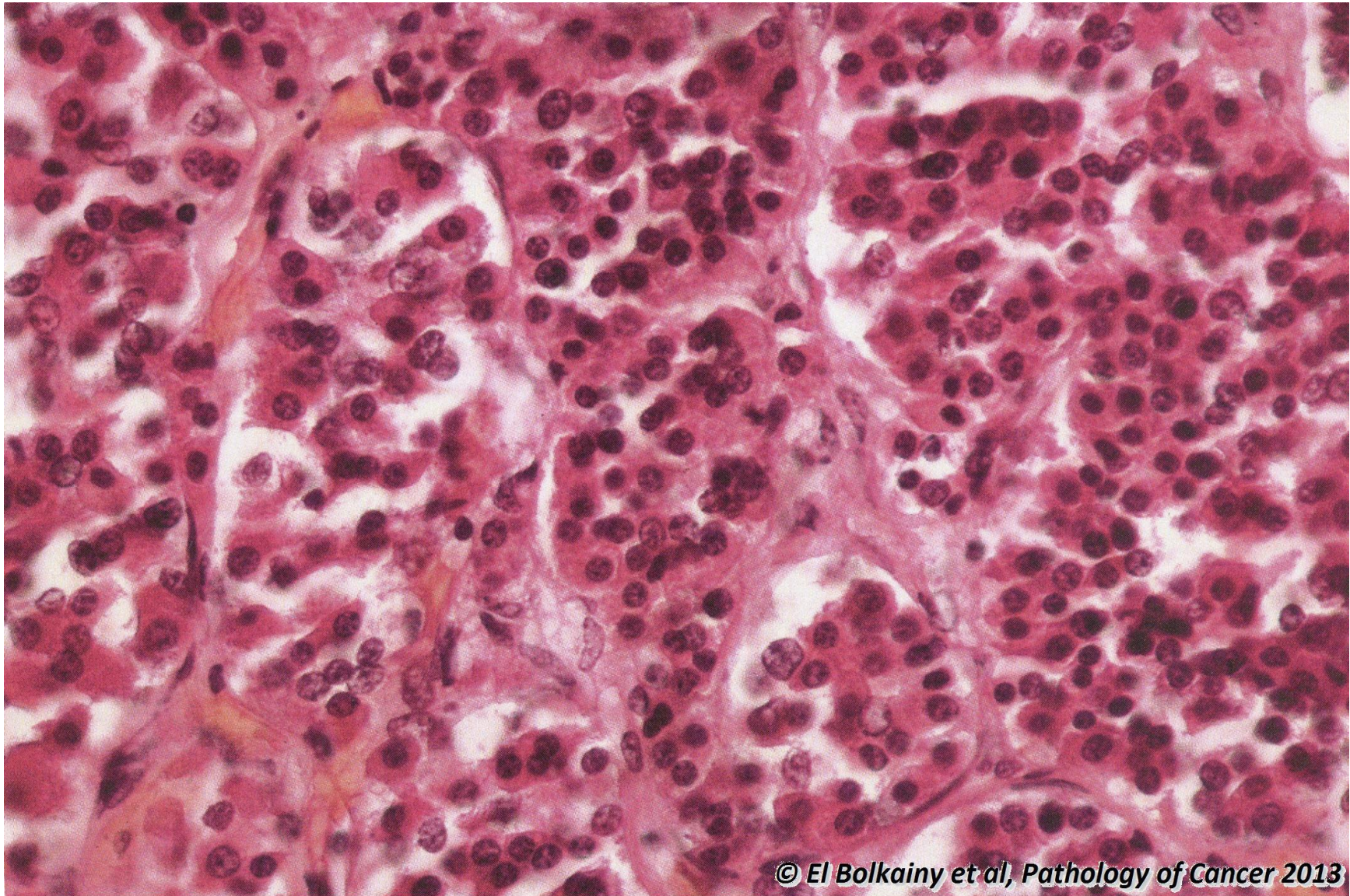
Picture 19-38 Adrenal cortical carcinoma, gross features. Large size (> 10 cm), yellow areas (lipid rich), brownish necrotic and reddish hemorrhagic areas. Invasion of perinephric fat may be evident.

19.39 Adrenal cortical carcinoma, histology.



Picture 19-39 Adrenal cortical carcinoma, histology. **A** Active mitosis ($> 2/\text{HPF}$). **B** Confluent massive necrosis and **C** angioinvasion. Immunoreactivity to vimentin, inhibin, melan-A, but negative for chromogranin and CD15.

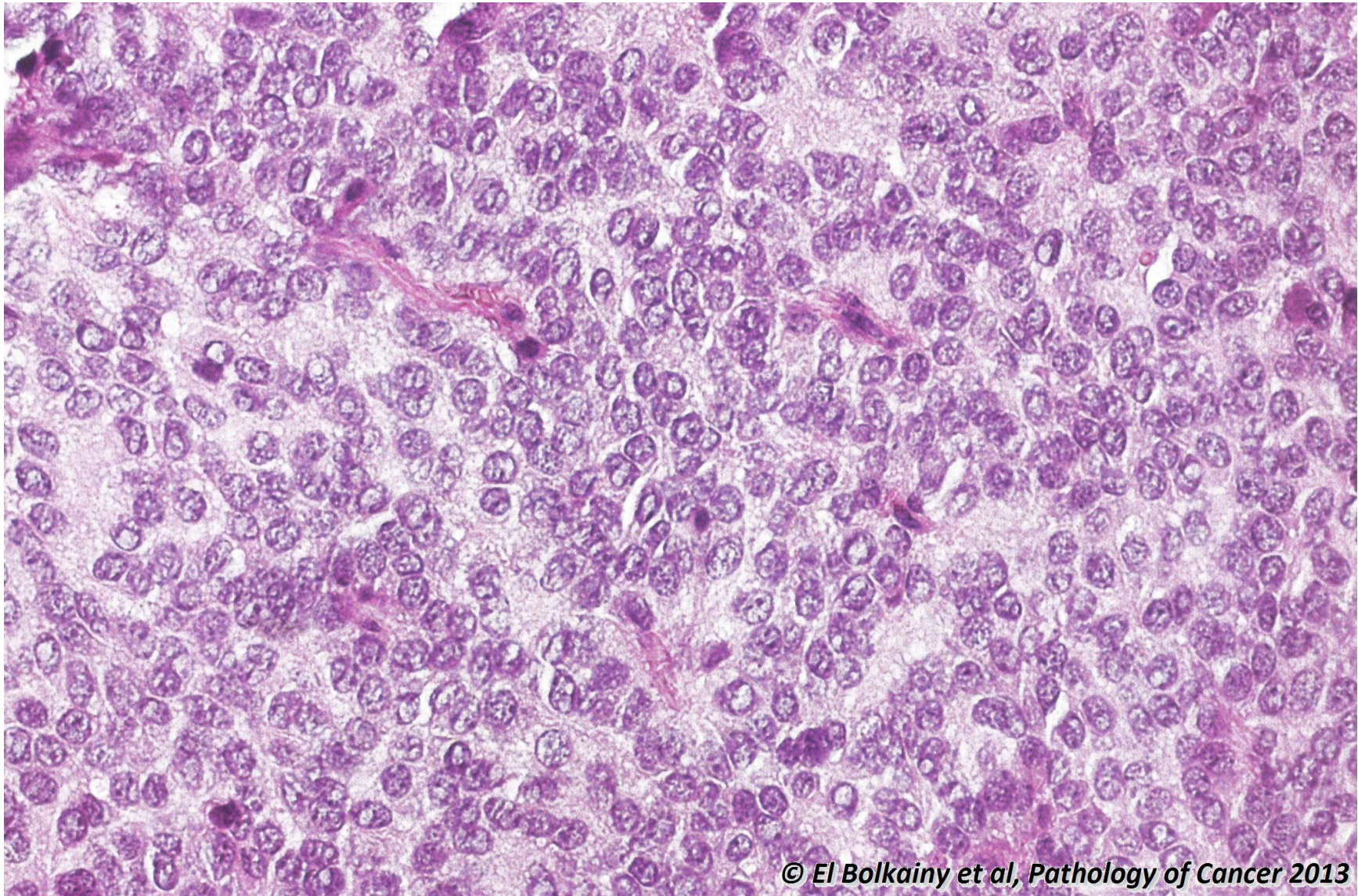
19.40 Anterior pituitary gland, growth-hormone producing adenoma.



© El Bolkainy et al, Pathology of Cancer 2013

Picture 19-40 Anterior pituitary gland, growth-hormone producing adenoma. It usually shows eosinophilic granules. Immunoreactivity to growth hormone. It is usually associated with acromegaly.

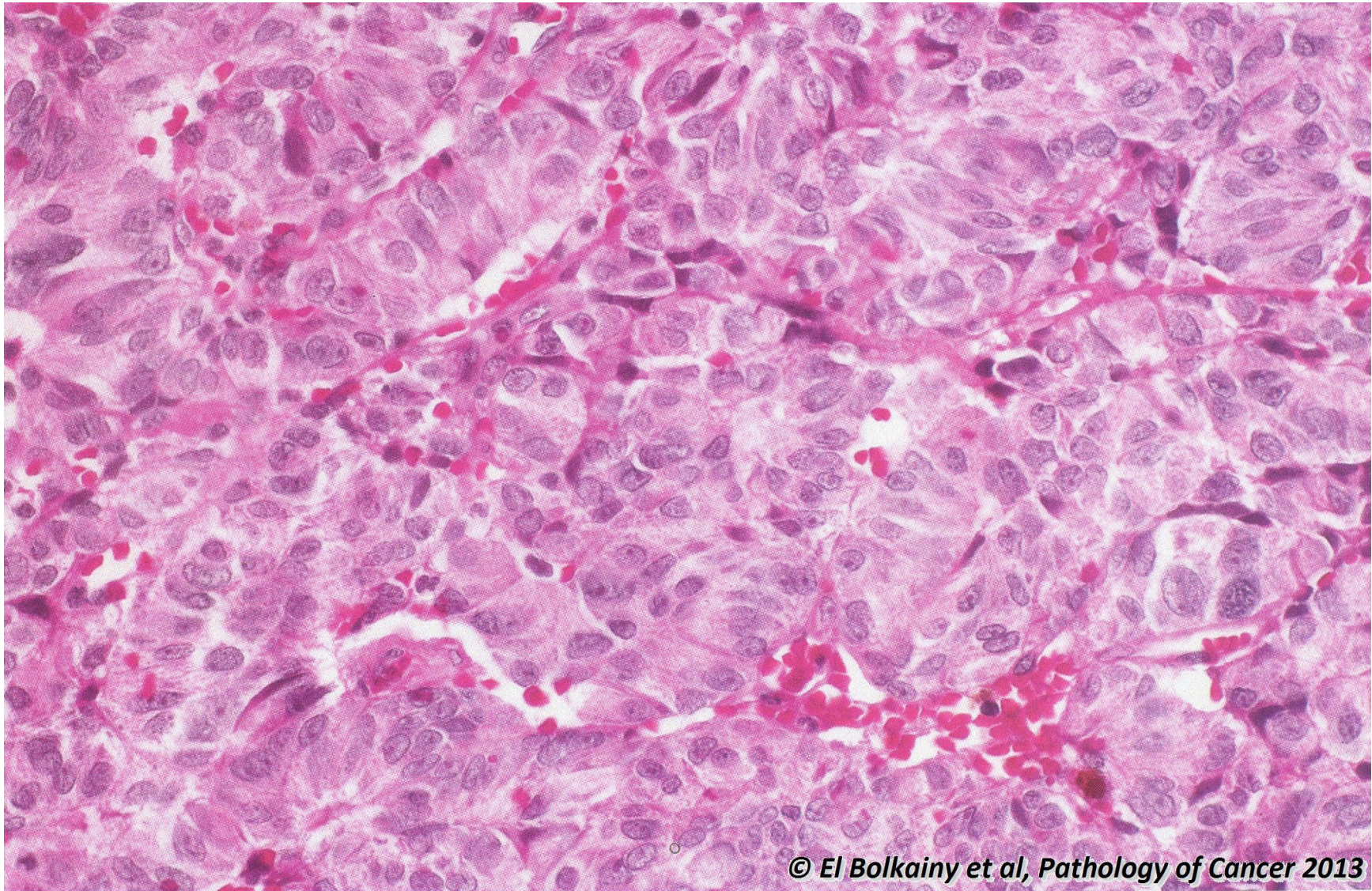
19.41 Anterior pituitary adenoma, prolactin producing.



© El Bolkainy et al, Pathology of Cancer 2013

Picture 19-41 Anterior pituitary adenoma, prolactin producing. It is the most common type, the cytoplasm is usually bluish in color (basophilic). About 50% are locally invasive. It is immunoreactive to prolactin.

19.42 Anterior pituitary null adenoma, histology.



© El Bolkainy et al, *Pathology of Cancer* 2013

Picture 19-42 Anterior pituitary null adenoma, histology. This is a non-functioning adenoma. The cells lack any granules and, hence, no immunoreactivity to all pituitary hormones. It is associated with hypogonadism and hypothyroidism.

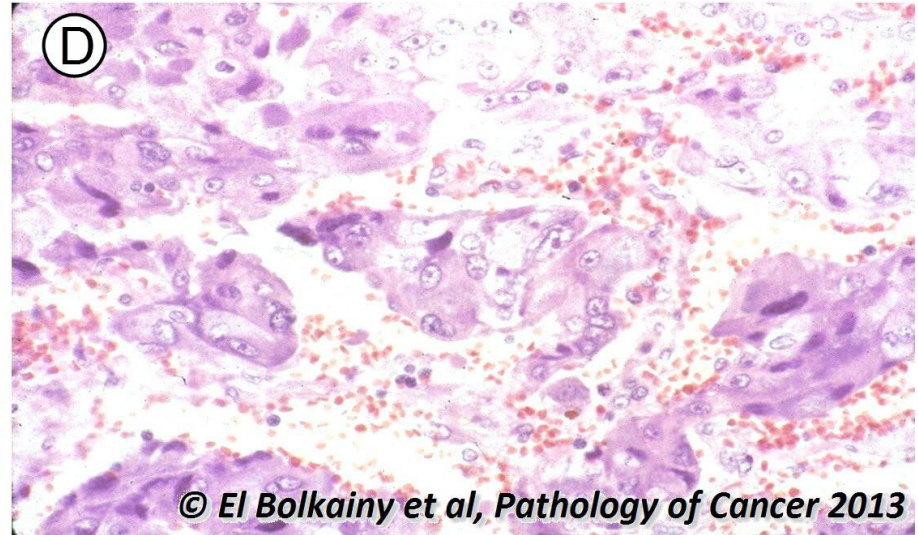
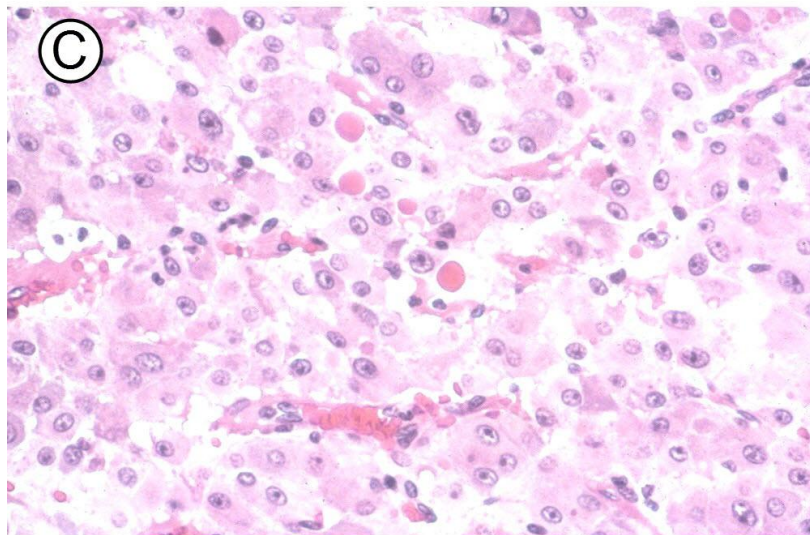
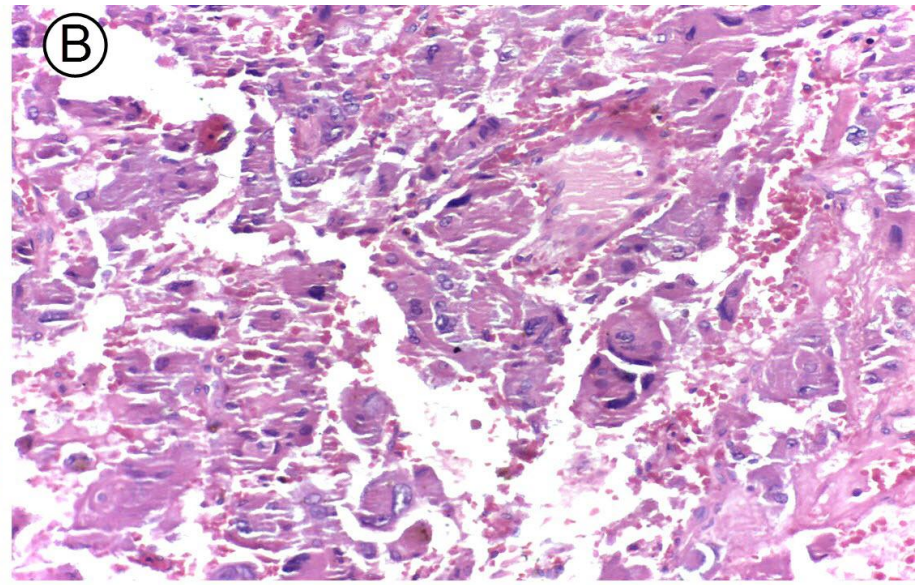
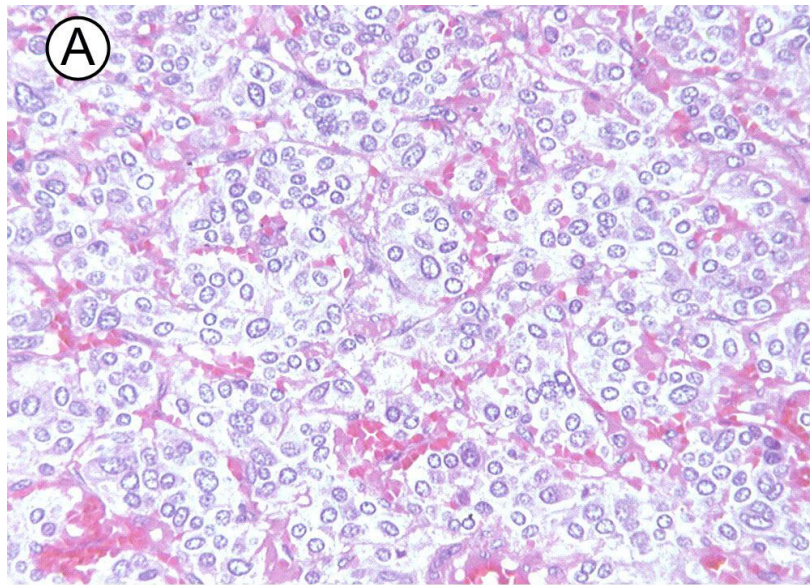
19.43 Adrenal pheochromocytoma, gross features.



© El Bolkainy et al, Pathology of Cancer 2013

Picture 19-43 Adrenal pheochromocytoma, gross features. Gray-brownish color, circumscribed and arising from medulla of adrenal gland which surrounds the gland. Mean tumor size 6cm in benign tumors and 10 cm in malignant tumors

19.44 Pheochromocytoma, histology.

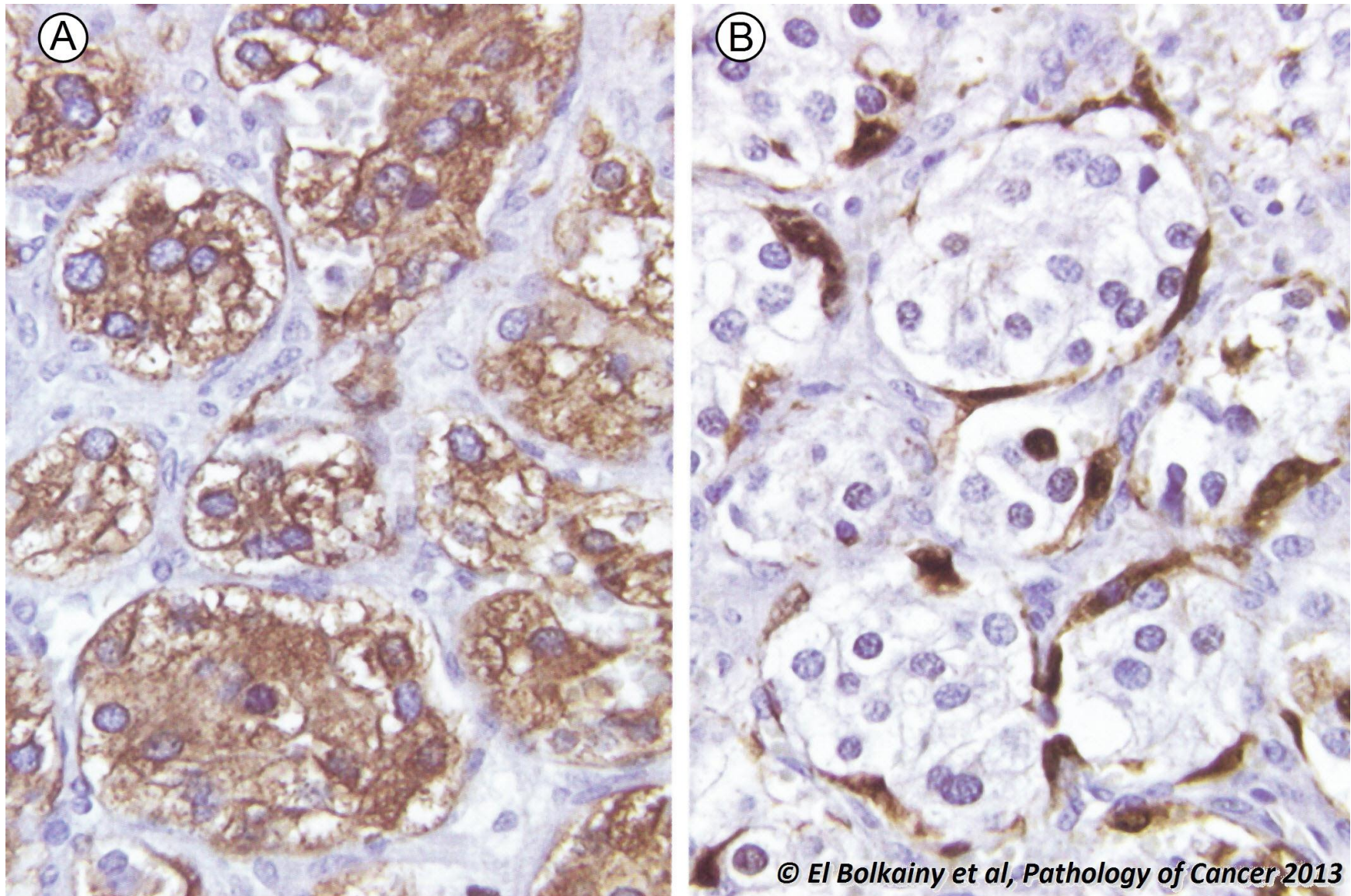


© El Bolkainy et al, Pathology of Cancer 2013

Picture 19-44

Pheochromocytoma, histology. A Nested pattern (Zellballen) in fibrovascular stroma. B Symplastic change. C Hyaline (PAS +ve) globules in cytoplasm and D cytoplasmic basophilia (bluish color).

19.45 Pheochromocytoma, immunophenotyping.

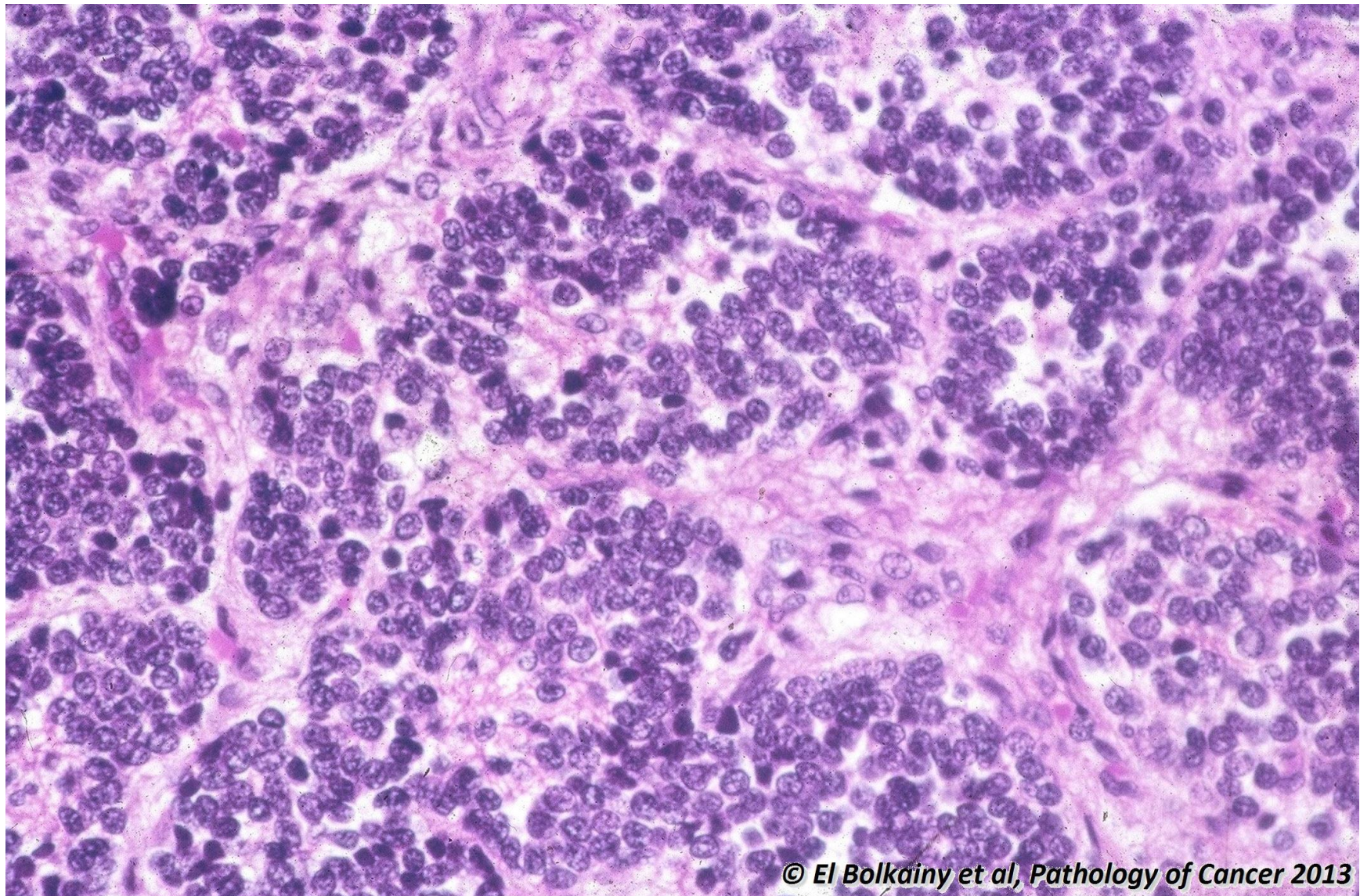


Picture 19-45

Pheochromocytoma, immunophenotyping. A Chromogranin positivity and B S-100 positive sustentacular cells in stroma. Contrary to adrenal cortical tumors, pheochromocytoma is negative for vimentin, inhibin, melan-A and cytokeratin.

© El Bolkainy et al, Pathology of Cancer 2013

19.46 Neuroblastoma, histology.

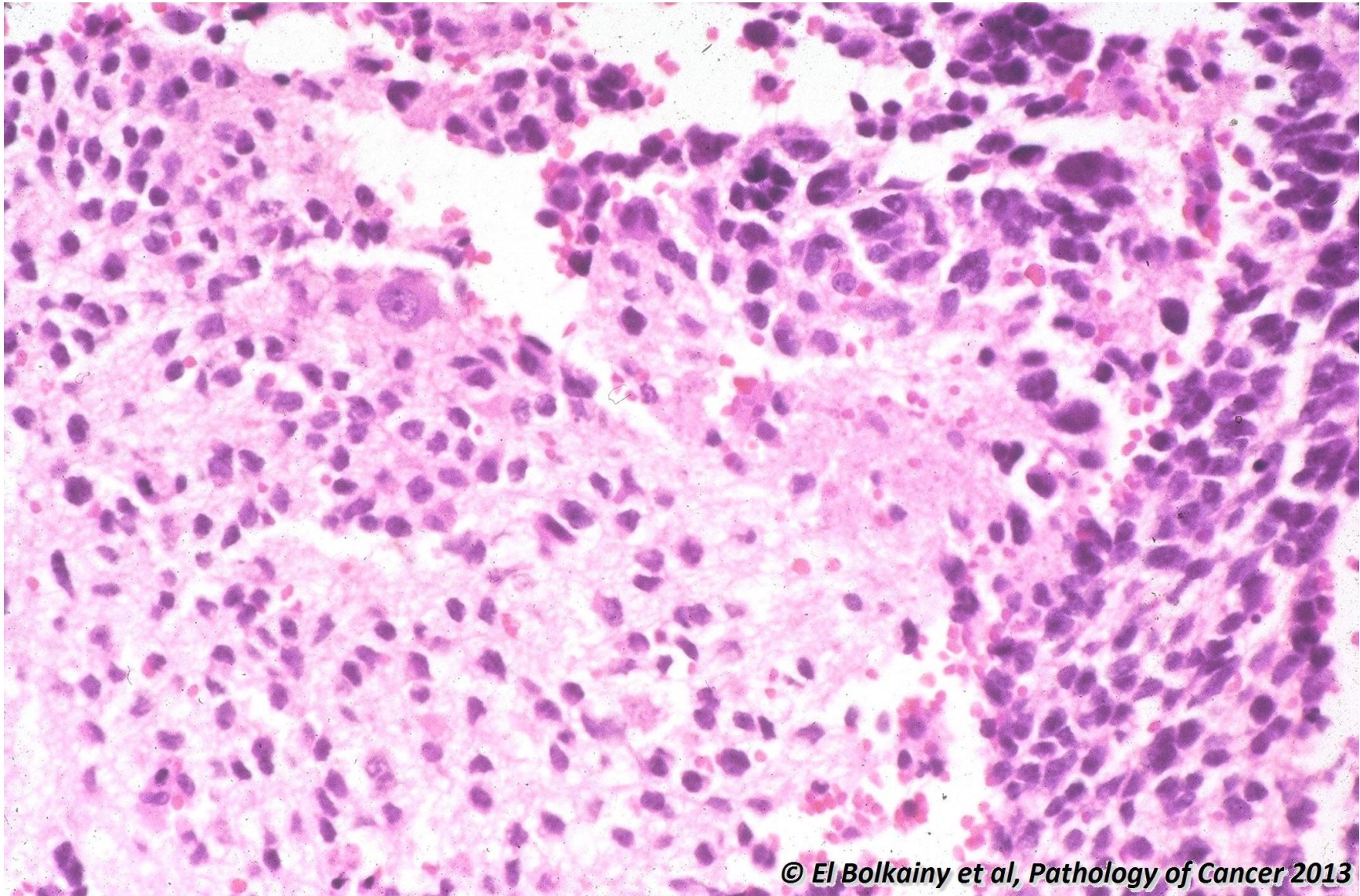


© El Bolkainy et al, Pathology of Cancer 2013

**Picture
19-46**

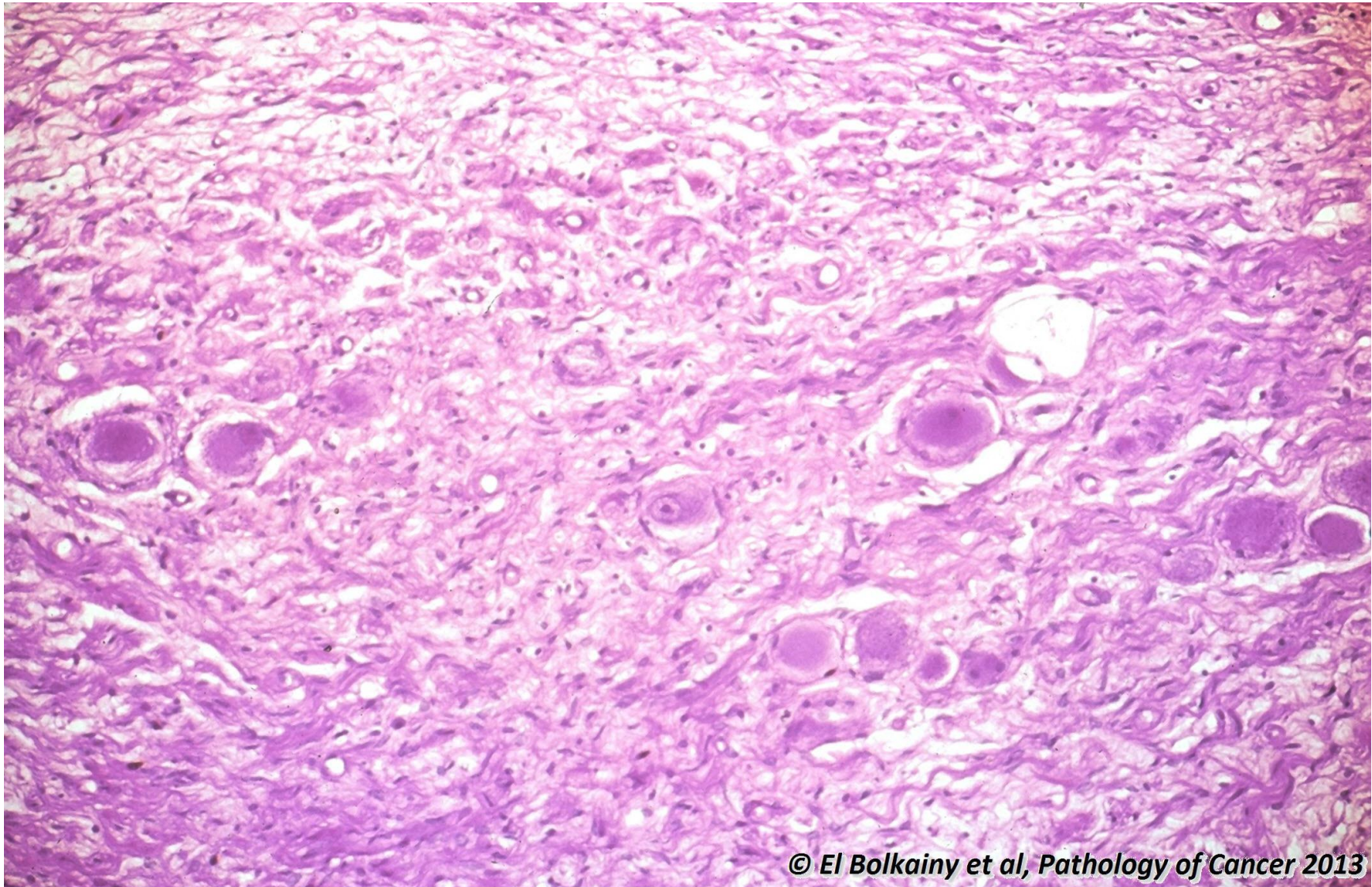
Neuroblastoma, histology. Groups of neuroblasts with pseudorosette pattern (Homer-Wright), surrounded by neuropil stroma (thin neuritic processes). Immunoreactivity: positive for chromogranin, but, negative for desmin and CD99.

19.47 Ganglioneuroblastoma, histology.



Picture 19-47 Ganglioneuroblastoma, histology. Ganglion cells with abundant cytoplasm are present (> 50%), but, still primitive neuroblasts are also evident.

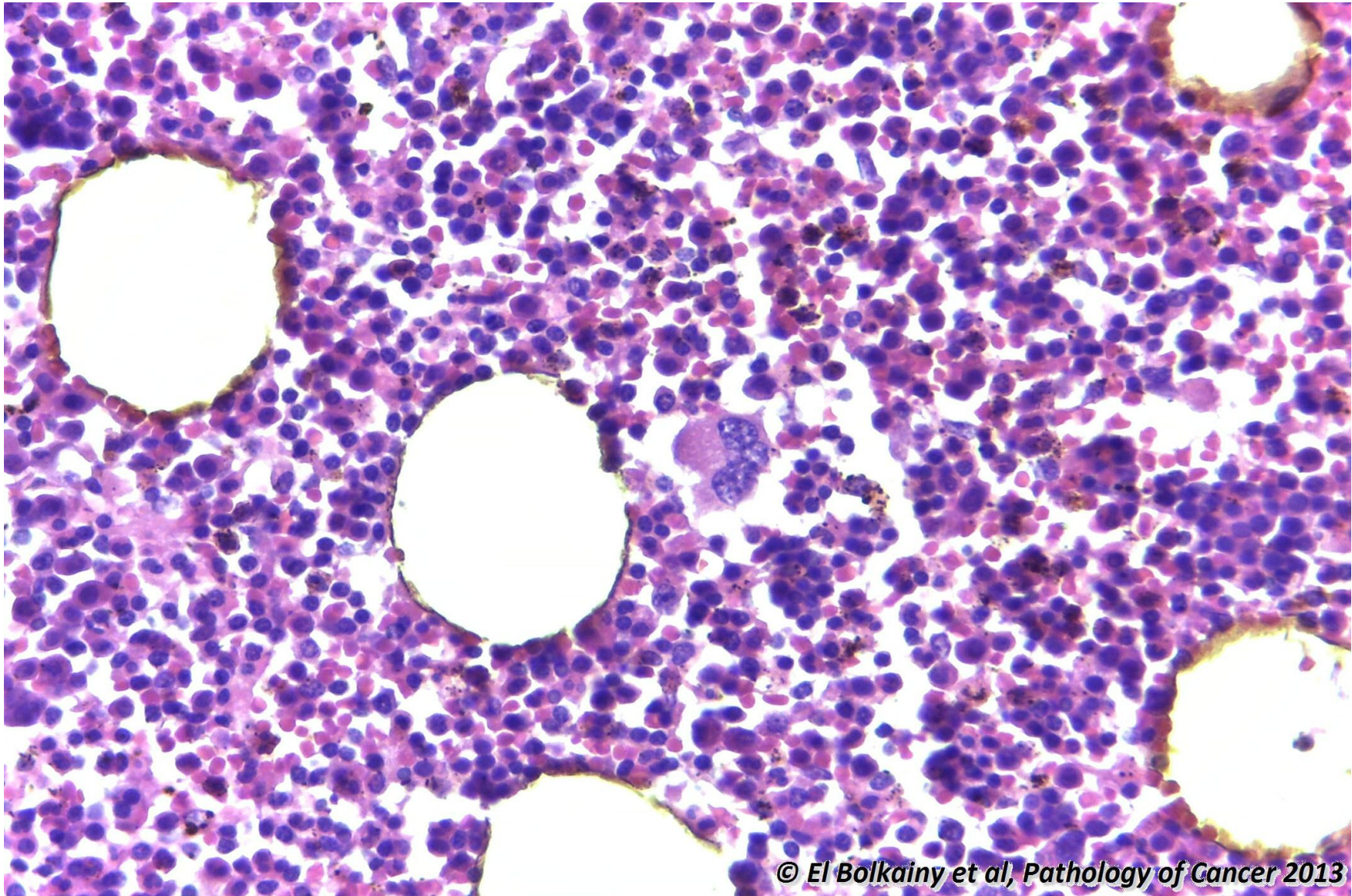
19.48 Ganglioneuroma, histology.



© El Bolkainy et al, Pathology of Cancer 2013

Picture 19-48 Ganglioneuroma, histology. Neurilemmal cell bundles predominate (S-100 positive) with focal groups of ganglion cells (synaptophysin positive).

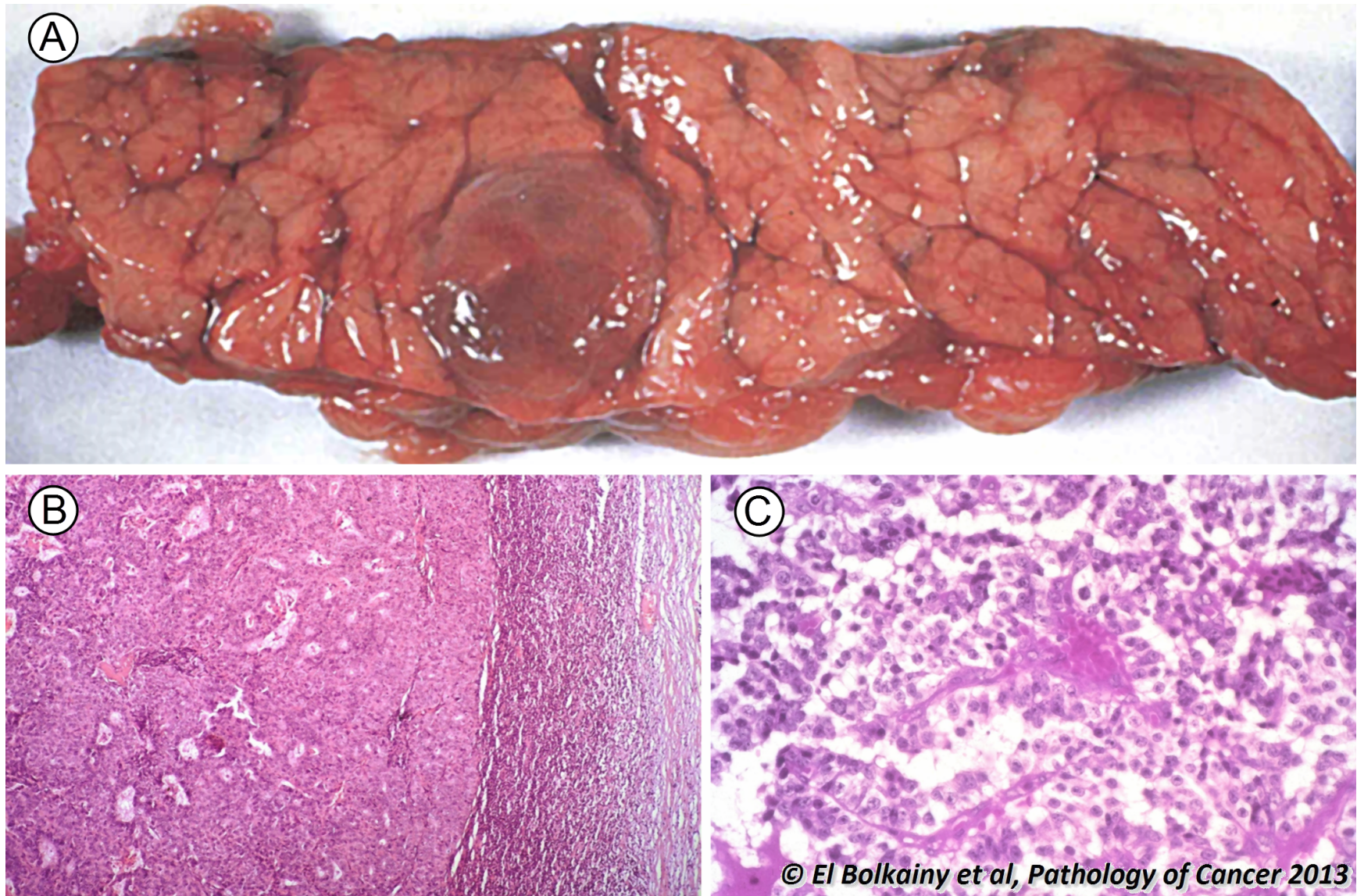
19.49 Adrenal myelolipoma, histology



**Picture
19-49**

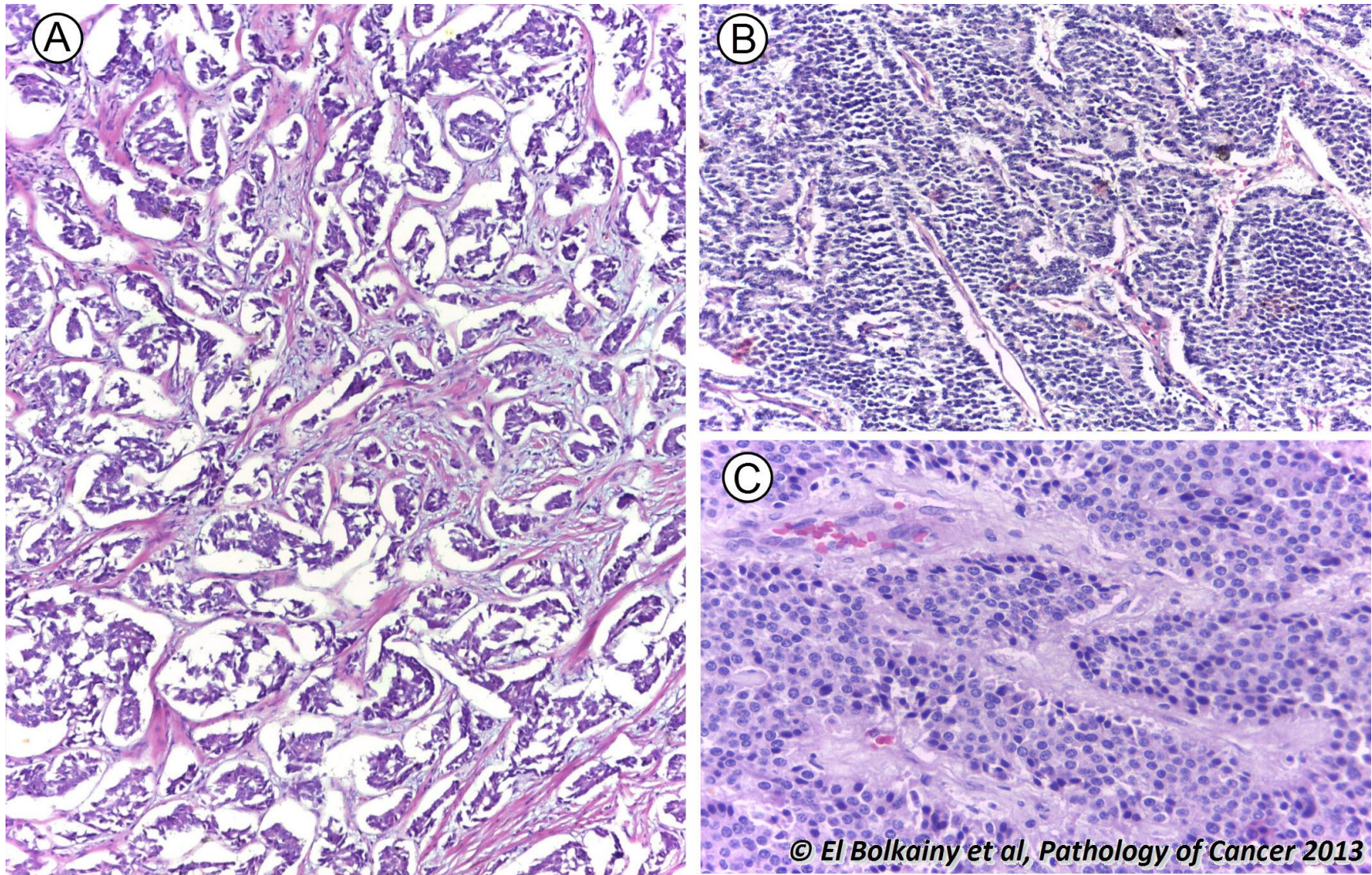
Adrenal myelolipoma, histology. It is composed of an admixture of mature fat cells and hematopoietic elements (trilineage maturation of myeloid, erythroid and megakaryocytic lines). It represents heterotopia and classified as a tumor-like lesion.

19.50 Pancreatic glucagonoma.



Picture 19-50 Pancreatic glucagonoma. **A** Gross features: a tumor mass arising in the body of pancreas. **B** The histology shows invasive insular pattern. About 90% of these tumors are malignant.

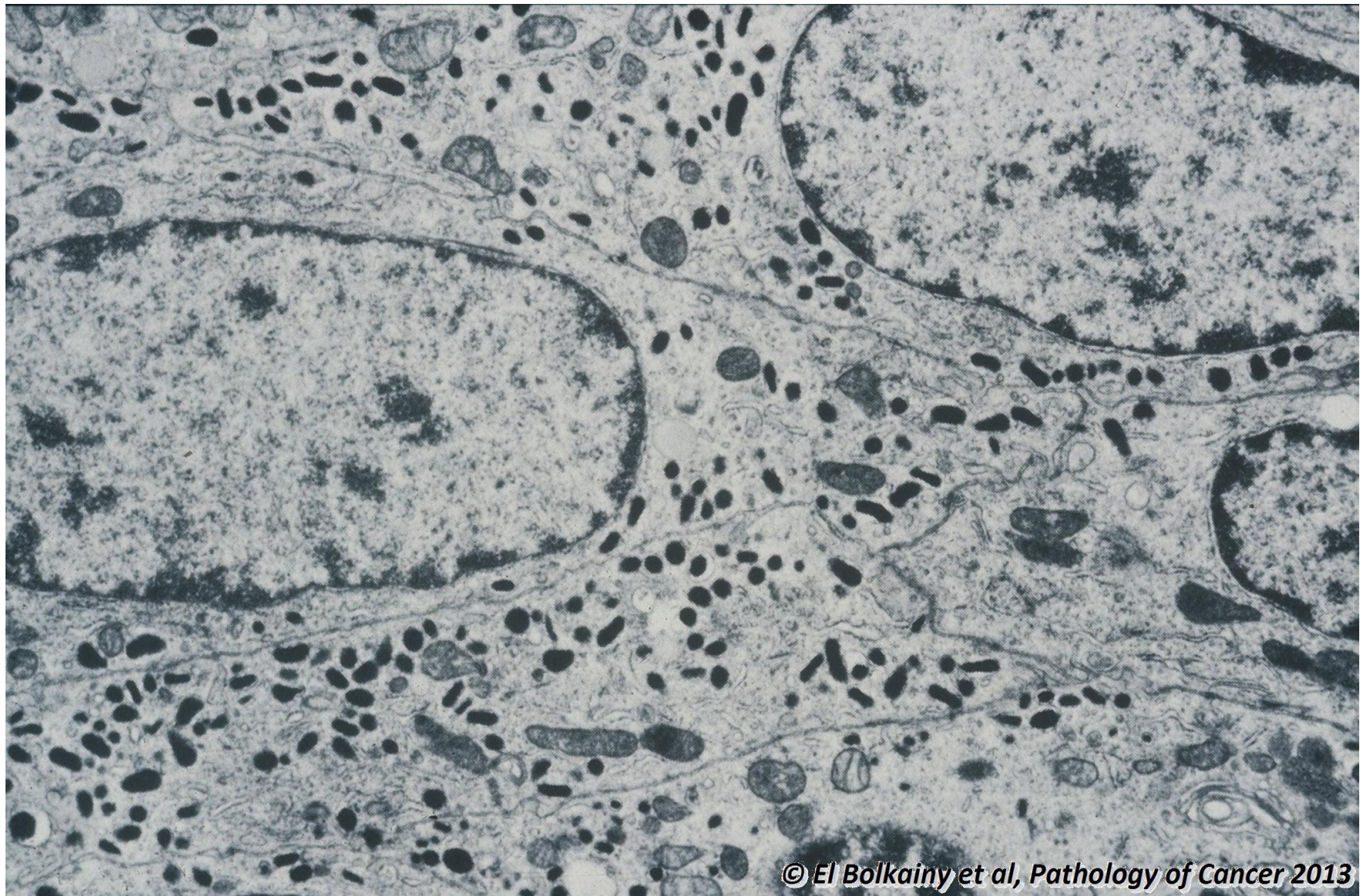
19.51 WHO classification of neuroendocrine tumors.



Picture 19-51

WHO classification of neuroendocrine tumors. A WHO grades I and II are histologically similar (< 2 mitosis/ 10 HPF) but different regarding the size. **B** Well-differentiated neuroendocrine carcinoma (>2 cm, 2-20 mitosis and necrosis). **C** Poorly differentiated neuroendocrine carcinoma (> 2 cm, > 20 mitosis and necrosis).

19.52 Neuroendocrine tumors, electron microscopy.



© El Bolkainy et al, Pathology of Cancer 2013

Picture 19-52 Neuroendocrine tumors, electron microscopy. Membrane-bound neurosecretory granules (size 100-400nm) are diagnostic of neuroendocrine differentiation.

